

Underlying mechanisms of two catalase-dependent apoptotic pathways in plasma-treated cancer cells

Charlotta Bengtson¹ and Annemie Bogaerts¹

¹ Research Group PLASMANt, Department of Chemistry, University of Antwerp,
Universiteitsplein 1, B-2610, Wilrijk-Antwerp, Belgium
email: charlotta.bengtson@uantwerpen.be

Cancer treatment by cold atmospheric plasma (CAP) offers the possibility to selectively eliminate cancer cells while leaving surrounding, normal cells, unaffected. The mechanisms underlying the CAP selectivity towards cancer cells are yet not fully understood, but based on experimental findings, it has been proposed that two apoptosis-inducing signaling pathways - which are inhibited by catalase - in the extracellular compartment are reactivated when catalase in the cell membrane of cancer cells is inactivated. Since CAP has the capacity to inactivate catalase, CAP may thus be used to induce cancer cell death by reactivation of these signaling pathways. A better insight of this specific apoptosis-inducing mechanism - especially the role of catalase inactivation - could be useful to increase our understanding of possible roles of CAP constituents in cancer treatment. In the present study, a mathematical model describing the reaction kinetics of the two apoptosis-inducing signaling pathways is developed and used to theoretically investigate their catalase-dependent reactivation. The results show that when only the reaction kinetics is considered, just one of the pathways may be responsible for apoptosis induction. This pathway requires a high catalase concentration (in the order of mM) to be inhibited, which thus can be assumed to be the condition of cancer cells before CAP treatment, and it can only be reactivated by inactivation of about 99% of the catalase. This model is a first step into the efforts that should be taken to quantitatively understand the complex mechanisms of the role of CAP and catalase in the apoptosis-inducing signaling pathways, but will need to be further extended before it can capture the entire mechanism. Still, it gives some important insights regarding necessary conditions in order for the proposed mechanism to represent a feasible explanation of selective CAP treatment of cancer cells.

Key words: Selective cancer treatment, cell signaling pathways, apoptosis-induction, cold atmospheric plasma, mathematical modeling.

1. Introduction

Recently, application of cold atmospheric plasma (CAP) on cancer tissue has emerged as a novel, promising cancer treatment, and up to now, CAP has shown significant effect in over 20 different types of cancer cell lines (*in vitro*) including brain cancer¹⁻², skin cancer³⁻⁵, breast cancer⁶⁻⁷, colorectal cancer⁸⁻⁹, lung cancer¹⁰⁻¹¹, cervical cancer¹²⁻¹³ and leukemia¹⁴⁻¹⁵. The first results from clinical application of CAP in cancer treatment are equally encouraging¹⁶⁻¹⁸. A special feature - and great advantage compared to most conventional cancer treatments - is the possibility to selectively eliminate cancer cells while leaving normal cells unaffected^{8, 10, 19-28}, although this selectivity is not always observed and depends on the treatment conditions²⁹.

It is generally accepted that the anti-cancer effect of CAP to a great extent is associated with reactive oxygen species (ROS) and reactive nitrogen species (RNS) generated in CAP. Especially, a rise of intracellular ROS in cancer cells (but not in normal cells) upon CAP treatment has been

reported^{22, 24, 30-32}. The significance of this intracellular rise of ROS has been experimentally verified by the observation that CAP treatment fails to eliminate cancer cells when these are pretreated with intracellular ROS scavengers^{2, 30-31}. Furthermore, CAP has been shown to trigger apoptosis in cancer cells *in vitro* and *in vivo*^{10, 33-42}. In the light of these findings, it has been argued that the anti-cancer effect of CAP is related to apoptosis-induction mediated by ROS and RNS^{30, 39, 41, 43-46}.

So far, most of the published work on the mechanisms underlying the anti-cancer effect of CAP is based on the idea that CAP contains ROS and RNS in sufficient concentration to induce apoptosis in cancer cells. However, a major change of concept - that accounts for selectivity in a very sophisticated manner - has been developed by Bauer and Graves³⁷. In this concept, CAP-generated ROS and RNS are believed to merely be the trigger to (re)activate apoptosis-inducing signaling pathways in the extracellular compartment of cancer cells. When (re)activated, these pathways thus transfer the signal to eliminate cells by self-destruction through apoptosis. Due to a difference in the extracellular compartment of cancer cells compared to normal cells, CAP will not trigger an activation of such apoptosis-inducing signaling pathways in normal cells - hence, the selectivity of CAP treatment. Recently, the first experiments evaluating this hypothesis were performed, with promising results⁴⁷⁻⁴⁸.

In the present study, we investigated the specific and detailed concept proposed in ref.³⁷, which is based on signaling pathways - originating from cell-derived species - occurring in the extracellular compartment of cancer cells. By mathematical modeling of the reaction kinetics of the apoptosis-inducing signaling pathways, which we believe is the core concept of the full mechanism, we analyzed and evaluated this hypothesis from a theoretical point of view and tried to reveal its range of applicability. The aim of this study is to contribute to the understanding of a potential underlying mechanism of the selective anti-cancer effect of CAP. As our model only contains a part of the full mechanism (the latter is more complicated, and also contains other CAP-associated mechanisms, such as the role of aquaporins and immune response), we cannot yet directly compare our results with the experiments of ref.⁴⁷, so this work is only a first step into investigating the proposed mechanism underlying the selective anticancer effect of CAP. We believe a stepwise model development approach, starting with a predictive model of the most essential components of the underlying mechanism, is an appropriate implementation as it allows to reject implausible scenarios along the way before increasing the complexity of the system. As a framework for the modeling, we first briefly discuss the apoptosis-inducing signaling pathways and how they are reactivated by CAP, and we present the motivation for this study as well as the explicit research questions.

2. Reactivation of apoptosis-inducing signaling pathways by CAP

Explicitly, the difference (of importance in this context) between cancer cells and normal cells, as briefly mentioned in the introduction, is to its simplest description based on two features that only cancer cells hold:

- Generation of extracellular superoxide anions.

- Membrane-associated catalase.

The extracellular superoxide anion generating enzyme NOX1 has been connected to cancer cell proliferation (i.e., the growth of cancer cells)⁴⁹⁻⁶⁰ and the generation of superoxide anions by several cancer cell lines has been reported⁶¹⁻⁶². Furthermore, there are studies showing that cancer progression requires the expression of membrane-associated catalase⁶³⁻⁶⁷. How these two features can be used to achieve selective cancer treatment by application of CAP is explained in the following three subsections.

2.1 Apoptosis-inducing signaling pathways originating from superoxide anions

The extracellular NOX1-generated superoxide anions are also the precursor of two apoptosis-inducing signaling pathways; the hypochlorous acid-pathway and the nitric oxide/peroxynitrite-pathway^{63-64, 68-70}. Together these pathways form what will be referred to as a *reaction network*. Both pathways in the reaction network result in the generation of hydroxyl radicals - a species causing apoptosis-induction through lipid peroxidation in the cell membrane. In the hypochlorous acid pathway, hydrogen peroxide is formed from superoxide anions in a reaction catalyzed by superoxide dismutase (SOD). Subsequently, hydrogen peroxide is used to synthesize hypochlorous acid in a reaction catalyzed by peroxidase (POD). Thereafter, hypochlorous acid reacts with superoxide anions to form hydroxyl radicals. In the nitric oxide/peroxynitrite pathway, superoxide anions first reacts with nitric oxide to form peroxynitrite. Subsequently, protonation of peroxynitrite forms peroxynitrous acid, which decomposes into nitrogen dioxide and hydroxyl radicals. For a schematic illustration of the two pathways in the reaction network, see Fig. 1.

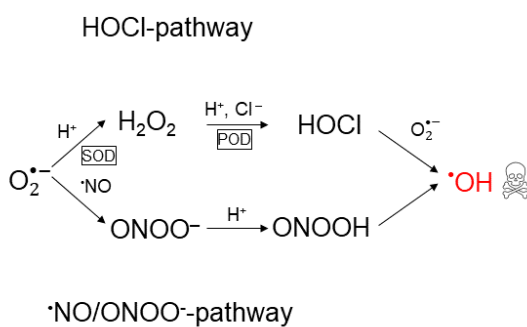


Fig. 1: Reaction network. Schematic illustration of the reaction network of apoptosis-inducing signaling pathways: the hypochlorous acid- and the nitric oxide/peroxynitrite pathway. Both pathways originate from superoxide anions and result in the formation of hydroxyl radicals which is responsible for apoptosis-induction.

2.2 The protective role of catalase

According to the concept in ref. ³⁷, the function of membrane-associated catalase in the extracellular compartment of cancer cells is to maintain the concentration of generated hydroxyl radicals below the threshold of apoptosis-induction. Extracellular membrane-associated catalase decomposes hydrogen peroxide into water and oxygen and thus removes the substrate for hypochlorous acid production ^{65, 67}. In addition, catalase can reduce the formation of peroxynitrite (through oxidation of nitric oxide ⁷¹) as well as decompose peroxynitrite into nitrite and oxygen ^{34, 67, 72}. Since the formation of peroxynitrite through reaction of nitric oxide and superoxide anions is very fast (much faster than the interaction between nitric oxide and catalase), it is reasonable to assume that the latter constitutes the major contribution to the peroxynitrite lowering effect of catalase. This conclusion was also drawn in e.g. ref. ³⁴. For a schematic illustration of the effect of catalase on the reaction network presented in Fig. 1, see Fig. 2. Since normal cells lack the generation of superoxide anions into the extracellular compartment, catalase is only expressed in the intracellular compartment (where ROS are generated from e.g. the mitochondria).

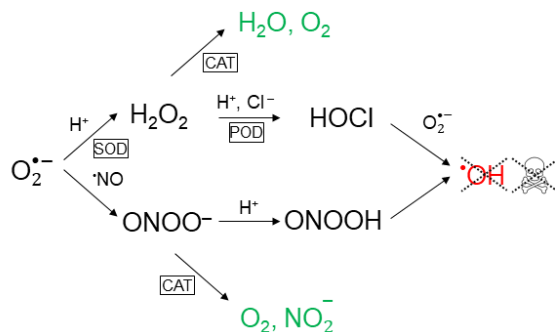


Fig 2: Reaction network with catalase. Catalase prevents the formation of hydroxyl radicals in both apoptosis-inducing signaling pathways. In the hypochlorous acid pathway, this occurs through decomposition of hydrogen peroxide into water and oxygen, and in the nitric oxide/peroxynitrite pathway it proceeds through decomposition of peroxynitrite into nitrite and oxygen.

2.3 Effect of CAP on cancer cells

According to ref. ³⁷, CAP causes (among others) selective cancer treatment due to its effect on catalase; it has been shown that singlet oxygen - which is one of the ROS known to be generated in CAP - has a strong potential to inactivate antioxidant enzymes, like catalase, through reaction with the histidine residues at the active centers ⁴². Thus, CAP may be used as a source of external singlet oxygen to inactivate the protective membrane-associated catalase in cancer cells. Applying CAP on tissue containing cancer cells will hence cause selective elimination of cancer cells

through reactivation of hydroxyl radicals generation from the hypochlorous acid- and the nitric oxide/peroxynitrite pathway in the extracellular compartment of these cells. A simplified cartoon picture of the events, forming the part that we believe is the core of the proposed mechanism of selective CAP treatment of cancer cells, can be seen in Fig. 3.

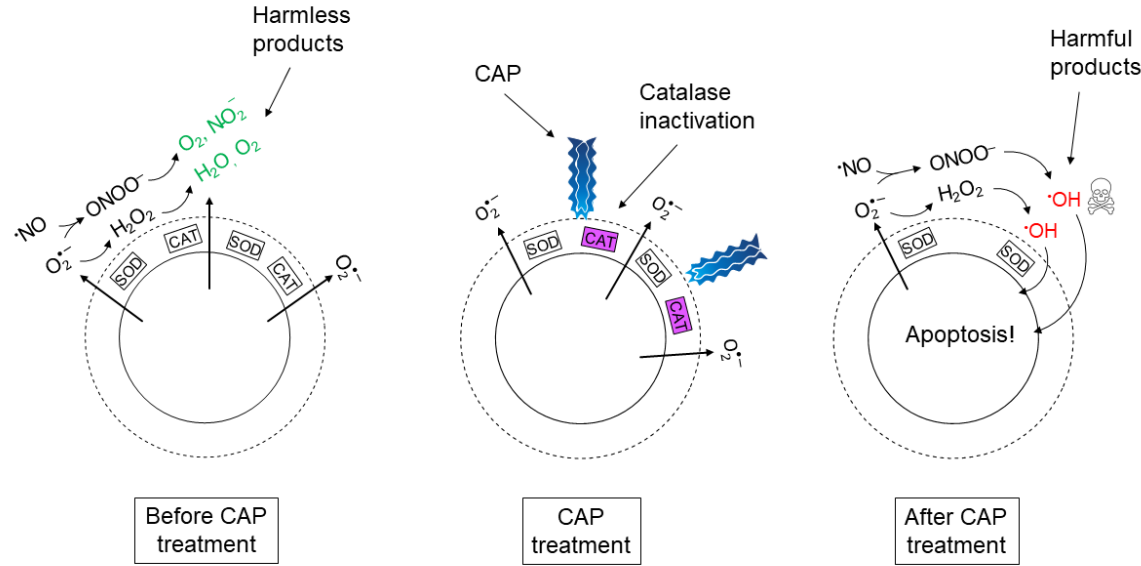


Fig. 3: Plasma cancer treatment. Proposed set of events underlying the mechanism of selective cancer treatment with CAP. The cartoon picture represents a cancer cell and its extracellular compartment before, during and after CAP treatment.

It should be noted that an important aspect of the full mechanism underlying the selectivity of cancer treatment by CAP as presented in ref. ³⁷, is the hypothesis that the non-decomposed hydrogen peroxide and peroxynitrite in the vicinity of inactivated catalase, may generate a burst of secondary singlet oxygen, which is propagated to adjacent cancer cells. In this catalase-dependent self-perpetuation of singlet oxygen, the effect of CAP is predicted to go beyond the surface of the cancer tumor, but the final effect on the bulk cancer cells is the same: inactivation of membrane-associated catalase and subsequent apoptosis-induction by the hypochlorous acid- and the nitric oxide/peroxynitrite pathway.

2.4 Motivation and research questions

Since a too high dose of CAP has been shown to cause cell death through necrosis rather than apoptosis - a process that is equally efficient in cancer cells as in normal cells ⁷³ - an important issue for the future use of CAP in cancer treatment is how to adjust the ROS and RNS concentration (and composition) of CAP such that it allows to selectively eliminate cancer cells through apoptosis induction. In the context of the concept proposed in ref. ³⁷ - which is the focus of the current study – this translates to determining in which regime CAP inactivates enough catalase to

reactivate hydroxyl radical generation in the extracellular compartment of cancer cells, but is well below the threshold for eliminating normal cells. The first step to accomplish this is of course to investigate how much catalase has to be inactivated in order to reactivate hydroxyl radical generation from the reaction network of the hypochlorous acid- and the nitric oxide/peroxynitrite pathway. This is the main motivation of our study.

So far, the effect of catalase on the hypochlorous acid- and the nitric oxide/peroxynitrite pathway has only been investigated experimentally. In other similar systems, mathematical modeling has proven to be a useful approach to increase the knowledge of the mechanisms of cell antioxidant defense and cell signaling, see e.g. refs. ⁷⁴⁻⁸⁶. An advantage of a mathematical model is that it allows to probe the system's behavior in ways that would not be possible in the lab. In the present study, a mathematical model of the kinetics of the proposed reaction network (catalase included) is developed and used to theoretically investigate the reactivation of the generation of hydroxyl radicals through inactivation of catalase. Numerical calculations are performed for various concentrations of catalase, to analyze the relationship between the catalase concentration and the generation of hydroxyl radicals. In particular, it is investigated to what extent catalase has to be inactivated in order for the hydroxyl radicals generation to be considered reactivated. The relationship between catalase inactivation and hydroxyl radicals generation in the reaction network of the hypochlorous acid- and the nitric oxide/peroxynitrite pathway is the specific research question that we seek to answer in this study.

3. The mathematical model

In this section, we present the construction and implementation of the mathematical model, describing the catalase-dependent kinetics of the reaction network in the extracellular compartment of cancer cells, and we point out the assumptions and simplifications underlying the model.

3.1 Construction of the mathematical model

Since this is the first attempt to construct a mathematical model of the reaction network of the hypochlorous acid- and nitric oxide/peroxynitrite pathways and its interaction with catalase, as our first simplification we choose to restrict the model to include the closed system of the reaction network (catalase-interaction included) itself only. Thus, any other possible interfering pathway or interaction with the surrounding is neglected. We admit that this model will not capture the full complexity of the kinetics of the reaction network in its *in vitro* or *in vivo* context, but we believe that it will provide fundamental insights about the kinetics of the reaction network itself and necessary conditions for catalase-dependent reactivation of hydroxyl radical generation. These insights can by extension be used as guidelines for further development of the model.

As a second simplification, we assume that the extracellular compartment of a cancer cell can be thought of as a well-mixed reaction vessel. All involved species are thus homogenously distributed, i.e., $\nabla^2 c_i = 0$, where c_i is the concentration of species i , for all (x, y, z) . The motivation for only considering the reaction kinetics is as follows: When the spatial dynamics is included in

a mathematical model of a reaction network, the rates of reactions of the different species in the network are competing with their diffusional loss. Since the important species in the reaction network all are located close to the cell membrane in the extracellular compartment, we can assume that the local concentration of especially enzymes is high and reactions should forestall diffusion. Thus, diffusion becomes less important since the species most probably will react before diffusing from the site of production. This assumption is justified by a number of studies for the two key species nitric oxide and superoxide anions ^{76-77, 87-88}. In these studies, the concentration of nitric oxide, superoxide anions and related species in the extracellular compartment of activated macrophages was investigated by mathematical modeling. Like cancer cells, macrophage cells generate both nitric oxide and superoxide anions into the extracellular compartment. In ref. ⁷⁷ it was estimated that superoxide anions are depleted within 1 μm above the cell surface and in ref. ⁷⁶ it was found that both superoxide anions and peroxy nitrite only exist in a very thin layer above the cell surface. In all these studies, nitric oxide reached the same steady-state concentration in the vicinity of the cells (despite different conditions such as cell density). Thus, in summary we are modelling the kinetics of the reaction network in a thin layer above the surface of *one* cancer cell as it would occur in a well-mixed reaction vessel.

Explicitly, the mathematical model is used to analyze the behavior of the dependent variable y , defined as

$$y(\bar{x}) = [\cdot\text{OH}]_{ss}^{\bar{x}}.$$

Here, \bar{x} denotes the set of independent variables that are varied in a particular system, which in our case is $[\text{CAT}]_0$, i.e., $\bar{x} = [\text{CAT}]_0$ and $[\text{CAT}]_0$ denotes the initial concentration of catalase, while $[\cdot\text{OH}]_{ss}^{\bar{x}}$ is the steady-state concentration of hydroxyl radicals (which is the dependent variable). In the numerical calculations, \bar{x} is given in per cent of $[\text{CAT}]_{0,\text{ref}}$, where $[\text{CAT}]_{0,\text{ref}}$ denotes the reference value of the catalase concentration, i.e., corresponding to the concentration of catalase in the extracellular compartment of a cancer cell before CAP treatment. Thus, we are focusing on how many per cent of the original catalase concentration has to be inactivated in order to reactivate hydroxyl radical generation.

We assume that the cellular generation rates of nitric oxide and superoxide anions exactly balance the rates of consumption before $t = 0$, i.e., the concentrations of nitric oxide and superoxide anions are constant (steady-state) before the disturbance of the kinetics by a change in the catalase concentration (due to the interaction between CAP and catalase). This disturbance is assumed to occur instantly at $t = 0$ and the effect in the kinetics is monitored thereafter. Thus, regarding the extracellular compartment as a reaction vessel in an experiment, the time $t = 0$ corresponds to the moment when the reaction vessel is prepared and the reading starts.

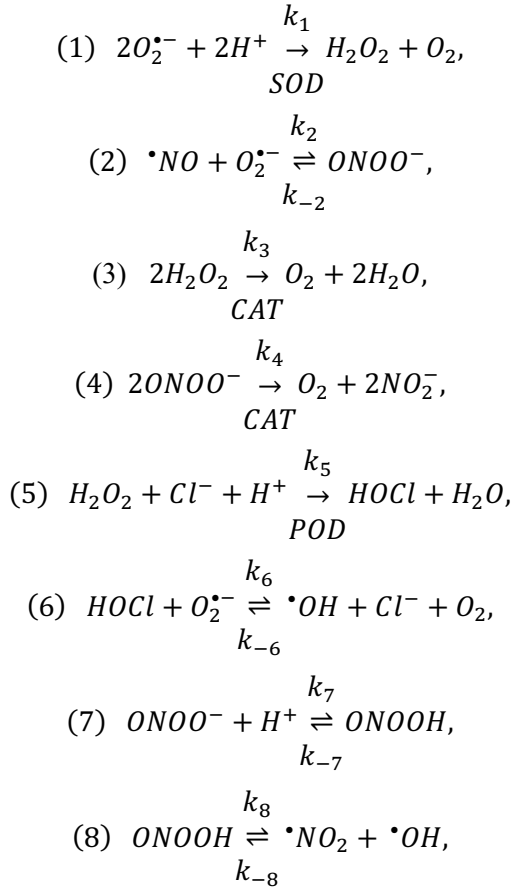
Ideally, the model should be compared and - if necessary - calibrated to experimental results, but to the best of our knowledge, there are no experimental studies for the catalase-dependency of the concentration of generated hydroxyl radicals in the extracellular compartment of cancer cells. Neither are there studies where an explicit correlation between the extracellular concentration of hydroxyl radicals and cancer cell apoptosis is reported - information that ultimately would be required as a reference value of when the hydroxyl radicals production can be considered

reactivated. For externally added hydroxyl radicals, the critical concentration to cause apoptosis-induction for lung cancer H460 cells, is around $0.3 \times 10^{16} \text{ cm}^{-3}$ ⁸⁹⁻⁹⁰. This corresponds to $[{}^{\bullet}\text{OH}] = 5 \times 10^{-6} \text{ M}$, which could be a value to refer back to when we evaluate our results.

It should be pointed out that in this study we do not consider *how* catalase is inactivated, i.e. if it is inactivated by primary singlet oxygen contained in CAP, secondary singlet oxygen generated by the cells themselves or any other species (e.g. superoxide anions or nitric oxide). Even though the generation of secondary singlet oxygen is a very important part of the full mechanism underlying selectivity of CAP cancer treatment, as proposed in ref.³⁷, taking the propagation of secondary singlet oxygen into account is beyond the scope of this study. Here, we are only concerned with the two apoptosis-inducing signaling pathways themselves and the impact of catalase-interference on their ability to generate hydroxyl radicals.

3.2 Reaction network

The reaction network, representing both apoptosis-inducing signaling pathways in the extracellular compartment of a cancer cell and their interaction with catalase, consists of the following reactions:



where k_i is the rate constant of the forward reaction for reaction (i) and k_{-i} is the rate constant for the backward reaction. Enzyme-catalyzed reactions are assumed to only proceed in the forward direction, in accordance with the assumptions for which experimental parameter values exist⁹¹⁻⁹².

Reaction (1), (3), (5) and (6) form the hypochlorous acid pathway, whereas reaction (2), (4), (7) and (8) form the nitric oxide/peroxynitrite pathway.

3.3 Rate equations

The kinetics of a reaction network is given by the set of rate equations describing the rate of production and consumption of each species in the network. Here, the explicit equations are summarized, as well as the assumptions made. A more detailed description of the rate equations and the references from where they have been taken, can be found in the Appendix (section A1).

Note that the reactions (1)-(8) are not elementary reactions, but rather consist of many different elementary reactions that we do not know about. The information available is the rate constants and reaction order for each species in the overall reaction, as they appear in experiments^{72, 91-102}. Hence, not all rate equations follow the law of mass action, but have other, experimentally observed, forms. More information is given in the Appendix, section A1.

We assume that $[H^+]$ is kept constant over time (due to a constant generation by proton pumps), i.e.,

$$\frac{d[H^+]}{dt} = 0.$$

Furthermore, we assume that $[Cl^-]$ is kept constant over time (due to a high physiological concentration compared to the other species), i.e.,

$$\frac{d[Cl^-]}{dt} = 0.$$

Finally, we assume that the catalysts, $[SOD]$, $[CAT]$ and $[POD]$, are kept constant over time, i.e.,

$$\frac{d[E]}{dt} = 0,$$

where E denotes SOD , CAT or POD .

The set of coupled rate equations, solving the time-dependence of the concentration of the different species, is then given by (see Appendix A1 for more details):

$$\begin{aligned}
\frac{d[O_2^{\bullet-}]}{dt} &= -[O_2^{\bullet-}](k_1[SOD] + k_2[\bullet NO] + k_6[HOCl]) + k_{-2}[ONOO^-] + k_{-6}[\bullet OH][Cl^-][O_2], \\
\frac{d[H^+]}{dt} &= 0, \\
\frac{d[H_2O_2]}{dt} &= \frac{1}{2}k_1[O_2^{\bullet-}][SOD] - [H_2O_2]\left(2k_3[CAT]_0\frac{1}{K_3 + [H_2O_2]} + k_5[POD]_0\frac{1}{K_5 + [H_2O_2]}\right), \\
\frac{d[\bullet NO]}{dt} &= -k_2[\bullet NO][O_2^{\bullet-}] + k_{-2}[ONOO^-], \\
\frac{d[ONOO^-]}{dt} &= k_2[\bullet NO][O_2^{\bullet-}] - [ONOO^-](k_{-2} + k_4[CAT] + k_7[H^+]) + k_{-7}[ONOOH], \\
\frac{d[Cl^-]}{dt} &= 0, \\
\frac{d[HOCl]}{dt} &= k_5[POD]_0\frac{[H_2O_2]}{K_5 + [H_2O_2]} - k_6[HOCl][O_2^{\bullet-}] + k_{-6}[\bullet OH][Cl^-][O_2], \\
\frac{d[\bullet OH]}{dt} &= k_6[HOCl][O_2^{\bullet-}] - [\bullet OH](k_{-6}[Cl^-][O_2] + k_{-8}[\bullet NO_2]) + k_8[ONOOH], \\
\frac{d[ONOOH]}{dt} &= k_7[ONOO^-][H^+] - [ONOOH](k_{-7} + k_8) + k_{-8}[\bullet NO_2][\bullet OH], \\
\frac{d[\bullet NO_2]}{dt} &= k_8[ONOOH] - k_{-8}[\bullet NO_2][\bullet OH], \\
\frac{d[SOD]}{dt} &= 0, \\
\frac{d[POD]}{dt} &= 0, \\
\frac{d[CAT]}{dt} &= 0.
\end{aligned}$$

Here, K_i is the Michaelis-Menten constant for reaction (i) .

Note that even though the set of rate equations are solved with respect to t , we are in this study not interested in the explicit time-dependence of each species but only the steady-state concentration of hydroxyl radicals as a function of the catalase concentration (see section 3.1).

4. Numerical details

In this section, we provide details of the numerical calculations, especially the parameter values used in the calculations.

4.1 Parameter values

The rate constants used in this study were collected from the literature, and in the case several different values were reported, the value that optimizes the production of hydroxyl radicals is used to create the upper limit for the hydroxyl radical production (see the Appendix, section A1, for more details).

The used rate constants for the non-enzyme catalyzed reactions, i.e. reaction (2), (6), (7) and (8), are summarized in Tab. 1. If not explicitly stated otherwise, the rate constants are for $T = 37^\circ\text{C}$ and $pH \sim 7$.

Tab. 1: Parameter values of the rate constants of the non-enzyme catalyzed reactions.

Rate constant	Value	Reference	Remark
k_2	$1.7 \times 10^{10} \text{ M}^{-1}\text{s}^{-1}$	⁹³	No information about pH .
k_{-2}	$17 \times 10^{-3} \text{ s}^{-1}$	¹⁰⁰⁻¹⁰¹	$T = 20 - 25^\circ\text{C}$
k_6	$7.5 \times 10^6 \text{ M}^{-1}\text{s}^{-1}$	⁹⁴	$T \sim 20^\circ\text{C}, pH = 5.5$
k_{-6}	0		Assigned
k_7	$10^{10} \text{ M}^{-1}\text{s}^{-1}$	⁹⁶	
k_{-7}	$k_7 K_a, pK_a = 6.8$	¹⁰²	
k_8	0.6 s^{-1}	⁹⁸	$T = 25^\circ\text{C}$, no information about pH .
k_{-8}	$3.5 \times 10^9 \text{ M}^{-1}\text{s}^{-1}$	⁹⁹	$pH = 9.5$, no information about T .

The used kinetic parameter values of the enzyme catalyzed reactions, i.e., reaction (1), (3), (4) and (5), are summarized in Tab. 2. If not explicitly stated otherwise, the parameter values are for *homo sapiens* and for $T = 37^\circ\text{C}$ and $pH \sim 7$.

Tab. 2: Parameter values of the rate constants and Michaelis-Menten constants of the enzyme catalyzed reactions.

Enzyme	Kinetic parameter	Reference	Remark
SOD	$k_1 = 2.35 \times 10^9 \text{ M}^{-1}\text{s}^{-1}$	^{95, 97}	Bovine, $T \sim 25^\circ\text{C}$
CAT _{H₂O₂}	$K_3 = 80.0 \times 10^{-3} \text{ M}$, $k_3 = 0.587 \times 10^6 \text{ s}^{-1}$	⁹¹	$[H_2O_2] \leq 200 \text{ nM}$
CAT _{ONOO⁻}	$k_4 = 1.7 \times 10^6 \text{ M}^{-1}\text{s}^{-1}$	⁷²	Bovine, $T = 25^\circ\text{C}$
POD	$K_5 = 30 \times 10^{-6} \text{ M}$, $k_5 = 320 \text{ s}^{-1}$	⁹²	$t \leq 100 \text{ ms}$

Since we wish to investigate the kinetics of the species truly originating from superoxide anions, i.e., without an external source of hydrogen peroxide, peroxynitrite, peroxynitrous acid, hypochlorous acid, hydroxyl radicals or nitrogen dioxide, all initial concentrations, except of $[O_2^{\cdot-}]_0$, $[^{\cdot}NO]_0$, $[H^+]_0$, $[Cl^-]_0$, $[CAT]_0$, $[SOD]_0$ and $[POD]_0$ were set to zero. The nonzero initial concentrations were taken from appropriate sources. We assumed $pH = 7$, i.e., $[H^+]_0 = 10^{-7} \text{ M}$. The used initial concentrations of the ROS and RNS are summarized in Tab. 3. The initial concentration of nitric oxide (ref. ¹⁰³) is an experimental value measured at the surface of a stimulated endothelial cell ($T = 37^\circ\text{C}$). This was the literature value found for conditions that best resemble ours. This value is also supported by other studies: for macrophages cells, the (steady-state) concentration of nitric oxide in the vicinity of the cells was $\sim 1 \mu\text{M}$ ^{77, 87-88}. The initial

concentration of superoxide anions (ref. ⁷⁶) is the steady state concentration of superoxide anions in the extracellular compartment of macrophage cells, which was found to be in the order of nM .

For the initial concentration of the enzymes in the extracellular compartment of cancer cells, no experimental values could be found. How this issue was dealt with is described in the results section.

Tab. 3: Initial concentrations of the ROS and RNS.

Species	Initial concentration (M)	Reference	Remark
$O_2^{\bullet-}$	10^{-9}	⁷⁶	
H^+	10^{-7}		Assigned
H_2O_2	0		Assigned
$\cdot NO$	10^{-6}	¹⁰³	In stimulated endothelial cells
$ONOO^-$	0		Assigned
Cl^-	0.140	¹⁰⁴	
$HOCl$	0		Assigned
$\cdot OH$	0		Assigned
$ONOOH$	0		Assigned
$\cdot NO_2$	0		Assigned

It should be noted that the parameter values used in this study were taken from experiments performed under conditions that most likely deviate in one or many aspects from the true *in vitro* or *in vivo* conditions in the extracellular compartment of a cancer cell. Having this in mind, we believe these parameter values are still a good starting point for the purpose of these numerical calculations.

4.2 Software and details about the calculations

The numerical calculations were performed in MATLAB. Due to significant differences in time scales, we used the solver `ode23s` to solve the set of rate equations.

In order to determine the most suitable time resolution and time scale for the calculations, we performed a number of test runs (fixed input parameter values), and we found on the time scale of 1 ms no significant difference in the calculation outcome for a single run with $[CAT]_0 = [CAT]_{0,\text{ref}}$ between using $dt = 1\text{ }\mu\text{s}$ (dt denoting the time resolution) as compared to $dt = 1\text{ ns}$. The same was true when $[CAT]_0 = 0\text{ M}$. Hence we determined that a time resolution of $1\text{ }\mu\text{s}$ yielded a result with desired accuracy. Since $[\cdot OH]$ reaches a steady-state on the 10 s - time scale when $[CAT]_0 = 0\text{ M}$ (and 100 ms when $[CAT]_0 = [CAT]_{0,\text{ref}}$ - the value of $[CAT]_{0,\text{ref}}$ will be discussed in section 5.1), we used $t_f = 10\text{ s}$ (t_f denoting the final time) in the calculations. Hence, we performed the numerical calculations for $dt = 1\text{ }\mu\text{s}$ and $t_f = 10\text{ s}$.

We varied the concentration of catalase according to $0 \leq [CAT]_0 \leq [CAT]_{0,\text{ref}}$ (see section 3.1), using interval steps, $\Delta [CAT]_0 = 0.01 [CAT]_{0,\text{ref}}$.

5. Results and discussion

5.1 Revealing the dominant signaling pathway for generation of hydroxyl radicals

Since we could not find experimental values for the concentration of the different enzymes in the extracellular compartment of cancer cells, we first performed a model analysis to assign feasible values for these parameters.

Information about the fate of superoxide anions - in particular which pathway contributes the most to the generation of hydroxyl radicals under the given conditions - can be extracted by considering the rates by which superoxide anions is consumed in the different pathways. The first reaction in each pathway is given by reaction (1) (the hypochlorous acid pathway) and (2) (the nitric oxide/peroxynitrite pathway). For short times, the rate, v_1 and v_2 , of superoxide anion consumption in each of these reactions is:

$$v_1 = -k_1[\text{O}_2^{\bullet-}]_0[\text{SOD}]_0,$$

$$v_2 = -k_2[\text{O}_2^{\bullet-}]_0[\bullet\text{NO}]_0.$$

The ratio of the initial rates is hence

$$\frac{v_2}{v_1} = \frac{k_2[\bullet\text{NO}]_0}{k_1[\text{SOD}]_0}.$$

Inserting the values of k_1 , k_2 and $[\bullet\text{NO}]_0$ (see Tab. 1, 2 and 3) yields

$$\frac{v_2}{v_1} \sim \frac{10^{-5}}{[\text{SOD}]_0}.$$

From this ratio of the initial consumption rates of superoxide anions in the two pathways, we can see that the value of $[\text{SOD}]_0$ (which is unknown) defines which one of three different regimes of the combined reaction network of the hypochlorous acid- and the nitric oxide/peroxynitrite pathway we are considering. Indeed, since the rate equation for SOD-catalyzed dismutation of superoxide anions is not given by a Michael-Menten equation (see ref. ⁹⁷), we are not constrained by the condition $[\text{SOD}]_0 \ll [\text{O}_2^{\bullet-}]$, but we can explore the whole regime of SOD-concentrations. The SOD-defined pathway regimes, according to this model and initial conditions, are:

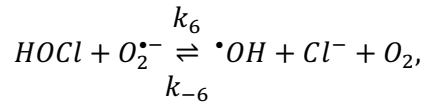
1. The nitric oxide/peroxynitrite pathway regime occurs for $[\text{SOD}]_0 \lesssim 10^{-7} \text{ M}$,
 $([\text{SOD}]_0 = 10^{-7} \text{ M} \Rightarrow v_2 \sim 100v_1).$
2. The combined pathway regime occurs for $10^{-7} \text{ M} \lesssim [\text{SOD}]_0 \lesssim 10^{-3} \text{ M}$.

3. The hypochlorous acid pathway regime occurs for $[SOD]_0 \gtrsim 10^{-3} M$,
 $([SOD]_0 = 10^{-3} M \Rightarrow v_1 \sim 100v_2)$.

If we assume that the SOD-molecules are solid spheres (in such a case their radius is in the order of $r = 16 \text{ \AA}$ - see Appendix, section A2), the volume that one SOD-molecule is occupying is given by a cube with the side length $2r$. The physical limit for the concentration of SOD is thus (N_A = Avogadro's constant):

$$[SOD]_{max} = \frac{1}{N_A} \frac{1}{8r^3} \sim 50 \times 10^{-3} M.$$

Thus, in order for the hypochlorous acid pathway to be dominant under the given conditions, the concentration of SOD has to be of the same order of magnitude as the physically maximal concentration of SOD. Moreover, since the generation of hydroxyl radicals in the hypochlorous acid pathway occurs through the reaction (i.e., reaction (6) in the reaction network in section 3.2)



there will not be a significant generation of hydroxyl radicals for this pathway, even in the regime where it is dominant. This can be seen by making an analysis of the rate of formation of hydroxyl radicals, which is given by

$$v'_6 = -v_6 = k_6 [HOCl]_t [O_2^{\cdot-}]_t,$$

where v_6 is the rate of superoxide anions consumption in reaction (6). The subscript t is used to emphasize that the concentrations no longer are at their initial values. Since superoxide anions is a precursor of hypochlorous acid, there is a trade-off between a high concentration of hypochlorous acid and a high concentration of superoxide anions. If $[CAT]_0 = 0$, then reaction (3) does not occur. If furthermore the nitric oxide/peroxynitrite pathway is neglected, i.e., reaction (2) is removed, then all superoxide anions will form hydrogen peroxide. Thus, the yield of hypochlorous acid is maximal. Furthermore, $k_{-6} = 0$ (see Tab. 1). In reaction (1) it can be seen that the stoichiometry is such that 2 moles of superoxide anions yield 1 mole of hydrogen peroxide. Reaction (5) reveals that 1 mole of hydrogen peroxide yields 1 mole of hypochlorous acid. At time t , the concentration of superoxide anions ($[O_2^{\cdot-}]_t$) will be the difference between the initial concentration of superoxide anions ($[O_2^{\cdot-}]_0$) and the fraction of the initial concentration of superoxide anions (f_t) that has been used in the formation of hypochlorous acid at time t ($[HOCl]_t$). Thus, $[O_2^{\cdot-}]_t = [O_2^{\cdot-}]_0 - f_t$. Since for each mole of formed hypochlorous acid, 2 moles of superoxide anions were required, $f_t = 2[HOCl]_t$, we get $[O_2^{\cdot-}]_t = ([O_2^{\cdot-}]_0 - 2[HOCl]_t)$. The rate v'_6 is hence a function of $[HOCl]_t$:

$$v'_6([HOCl]_t) = -k_6 [HOCl]_t ([O_2^{\cdot-}]_0 - 2[HOCl]_t).$$

If we for now denote $[HOCl]_t = x$ and $[O_2^{\bullet-}]_0 = c_0$ in the derivation, then the rate of formation of hydroxyl radicals is given by:

$$\nu'_6(x) = k_6 x(c_0 - 2x) = k_6 x c_0 - 2k_6 x^2.$$

Furthermore,

$$\frac{d\nu'_6}{dt} = k_6 c_0 - 4k_6 x,$$

and

$$\frac{d^2\nu'_6}{dt^2} = -4k_6 < 0.$$

The maximum (since $\frac{d^2\nu'_6}{dt^2} < 0$), of the rate of formation of hydroxyl radicals is thus given by

$$\frac{d\nu'_6}{dt} = 0 \Rightarrow k_6 c_0 - 4k_6 x_{max} = 0 \Leftrightarrow x_{max} = \frac{c_0}{4}.$$

Hence, the function ν'_6 has a maximum, $\nu'_{6,max}$, at

$$[HOCl]_{t,max} = \frac{[O_2^{\bullet-}]_0}{4}.$$

The ratio between the rate of superoxide anions consumption in reaction (1) and reaction (6) at time (t) is ($[SOD]_t = [SOD]_0$)

$$\frac{\nu_1}{\nu_6} = \frac{k_1 [SOD]_0}{k_6 [HOCl]_t}.$$

Inserting $[HOCl]_{t,max}$ and the values of k_1 and k_6 (see Tab. 1 and 2) yields

$$\frac{\nu_1}{\nu_{6,max}} = \frac{4k_1 [SOD]_0}{k_6 [O_2^{\bullet-}]_0} \sim \frac{10^3 [SOD]_0}{[O_2^{\bullet-}]_0}.$$

In order for these two reactions to occur at approximately the same rate (given that $[O_2^{\bullet-}]_0 = 10^{-9} M$, see Tab. 3), $[SOD]_0 \sim 10^{-12} M$. In such a case, in order for reaction (1) and (2) to occur at approximately the same rate, $[\bullet NO]_0$ has to be several orders of magnitude smaller than the value reported in Tab. 3. In fact, $[\bullet NO]_0 \sim 10^{-13} M$.

For $[SOD]_0 \sim 10^{-3} M$ (the hypochlorous acid pathway regime), $\nu_1 \sim 10^9 \nu_{6,max}$, i.e., the generation of hydroxyl radicals from reaction (6) is negligible. Hence, the kinetics of the reaction network suggests that the hypochlorous acid pathway regime is insignificant regarding the possibility to reactivate hydroxyl radicals generation.

For the second regime, where both pathways come into play, the same reasoning applies; there will not be a significant amount of hydroxyl radicals generated from the hypochlorous acid pathway and any superoxide anions going into the hypochlorous acid pathway will decrease the total hydroxyl radicals production of the reaction network. Thus, the interesting regime to investigate is the first regime where the nitric oxide/peroxynitrite pathway operates alone.

Regarding the nitric oxide/peroxynitrite pathway alone (i.e., $[SOD]_0 \lesssim 10^{-7} M$) the only enzyme-catalyzed reaction (with catalase) is not given as a Michaelis-Menten mechanism (see ref.⁹¹), so in this case it should be feasible to use the physically maximal concentration of catalase as $[CAT]_{0,ref}$ (see section 3.1) to explore the whole regime of possible catalase concentrations. We thus used the concentration of catalase when the whole extracellular compartment is maximally filled with catalase as our default reference value. This concentration was found in the same manner as in the case of SOD. The radius is now $r = 25 \text{ \AA}$ (see Appendix, section A2) which yields $[CAT]_{0,max} \sim 10^{-2} M$.

5.2 The catalase-dependence of the generation of hydroxyl radicals in the nitric oxide/peroxynitrite pathway

Since it has been shown in the previous section that virtually no hydroxyl radicals is generated from the hypochlorous acid pathway in this model (even when the condition $[SOD] \gtrsim 10^{-3} M$ is fulfilled), we have chosen to exclude the hypochlorous acid pathway from the numerical calculations and instead we focused solely on the nitric oxide/peroxynitrite pathway.

Fig. 4 illustrates the steady state hydroxyl radical concentration, $y(\bar{x})$, as a function of the catalase concentration, \bar{x} , more specifically as % of $[CAT]_{0,ref}$.

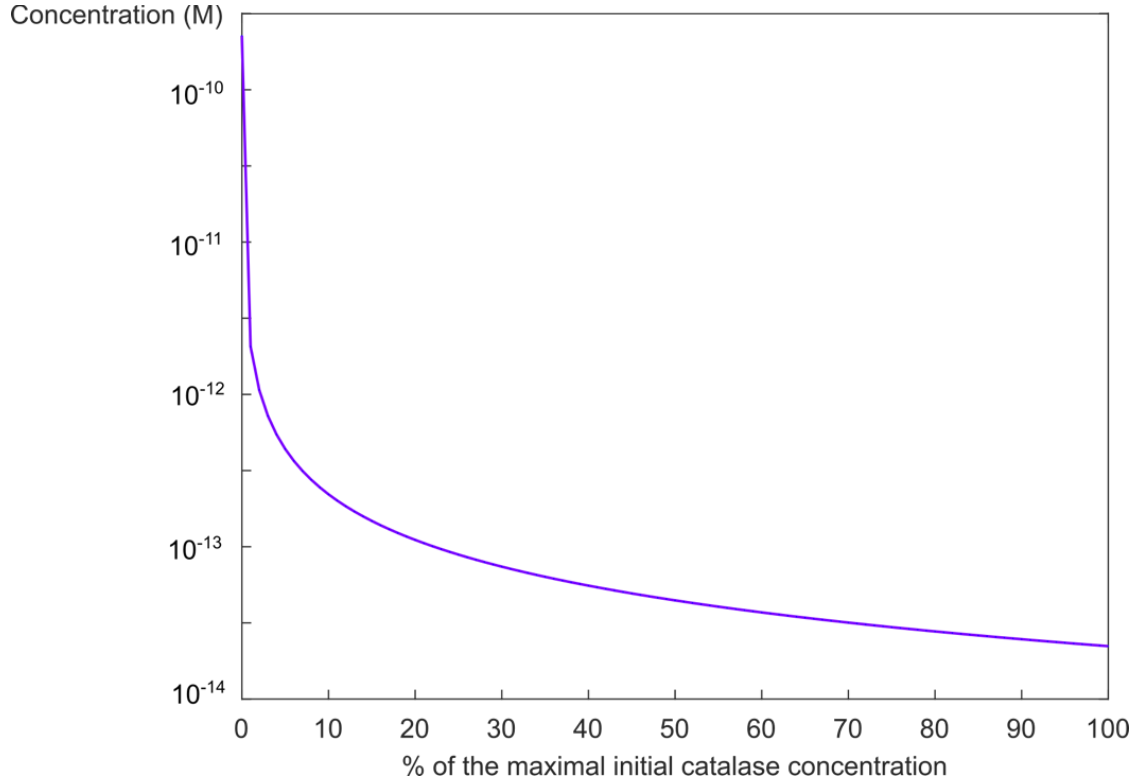


Fig 4: Hydroxyl radical concentration as a function of catalase concentration. The catalase concentration is given as % of a reference value, which in this calculation was $10^{-2} M$ (see section 5.1 above).

Assuming that $[CAT]_0 = 0$ corresponds to a fully reactivated pathway, we can see that a catalase concentration of 10% of $[CAT]_{0,ref}$, reduces $[\cdot OH]$ by three orders of magnitude (from $[\cdot OH] \sim 10^{-9.6} M = 2.5 \times 10^{-10} M$ to $[\cdot OH] \sim 10^{-12.7} M = 2.0 \times 10^{-13} M$). For catalase concentrations $0.1[CAT]_{0,ref} \leq \bar{x} \leq [CAT]_{0,ref}$, on the other hand, $[\cdot OH]$ only drops by about one order of magnitude. Therefore, it should be reasonable to assume that the catalase concentration in the extracellular compartment of cancer cells (before CAP treatment) is about 1 mM or more. Indeed, this concentration seems to significantly reduce the hydroxyl radical concentration, and thus protects cancer cells from apoptosis. For a (nearly) fully reactivated pathway, most of the catalase needs to be inactivated.

Based on the above conclusion, new calculations with $[CAT]_{0,ref} = 1 mM$ were performed. The result can be seen in Fig. 5. This plot looks very similar to that shown in Fig. 4; again, $\left| \frac{dy}{dx} \right|$ is larger for smaller \bar{x} and in the region of $\bar{x} \leq 0.1[CAT]_{0,ref}$, the concentration of hydroxyl radicals drops by about two orders of magnitude (from $[\cdot OH] \sim 10^{-9.6} M = 2.5 \times 10^{-10} M$ to $[\cdot OH] \sim 10^{-11.7} M = 2.0 \times 10^{-12} M$), whereas in the region $0.1[CAT]_{0,ref} \leq \bar{x} \leq [CAT]_{0,ref}$ it only drops by about one order of magnitude. Still, for a (nearly) fully reactivated pathway, approximately 99% of the catalase has to be inactivated. In ref.¹⁰⁵ it is shown that in experiments with catalase in solution, the concentration has to be very high in order to inactivate the nitric oxide/peroxynitrite pathway. Hence, our model seems to reproduce this experimental result.

Additional calculations with $[CAT]_{0,ref} = 1 \mu M$ were also performed. This result can be seen in Fig. 6. A catalase concentration of $1 \mu M$ only lowers the generated hydroxyl radicals by less than one order of magnitude and is thus not enough to protect the cancer cell from the nitric oxide/peroxynitrite pathway.

Comparing the concentration of generated hydroxyl radicals at $[CAT]_0 = 0 M$ (i.e., $[^\bullet OH] = 2.5 \times 10^{-10} M$) with the experimental result in ref.⁸⁹⁻⁹⁰ (i.e., critical hydroxyl radical concentration for apoptosis-induction, $[^\bullet OH] = 5 \times 10^{-6} M$, as mentioned in section 3.1), we can see that when hydroxyl radicals is added externally, a concentration almost four orders of magnitude higher is required to induce apoptosis. However, since hydroxyl radicals is a highly reactive species, the effective $[^\bullet OH]$ at locations where it can lead to lipid peroxidation (and thus, apoptosis), might be much lower when added externally.

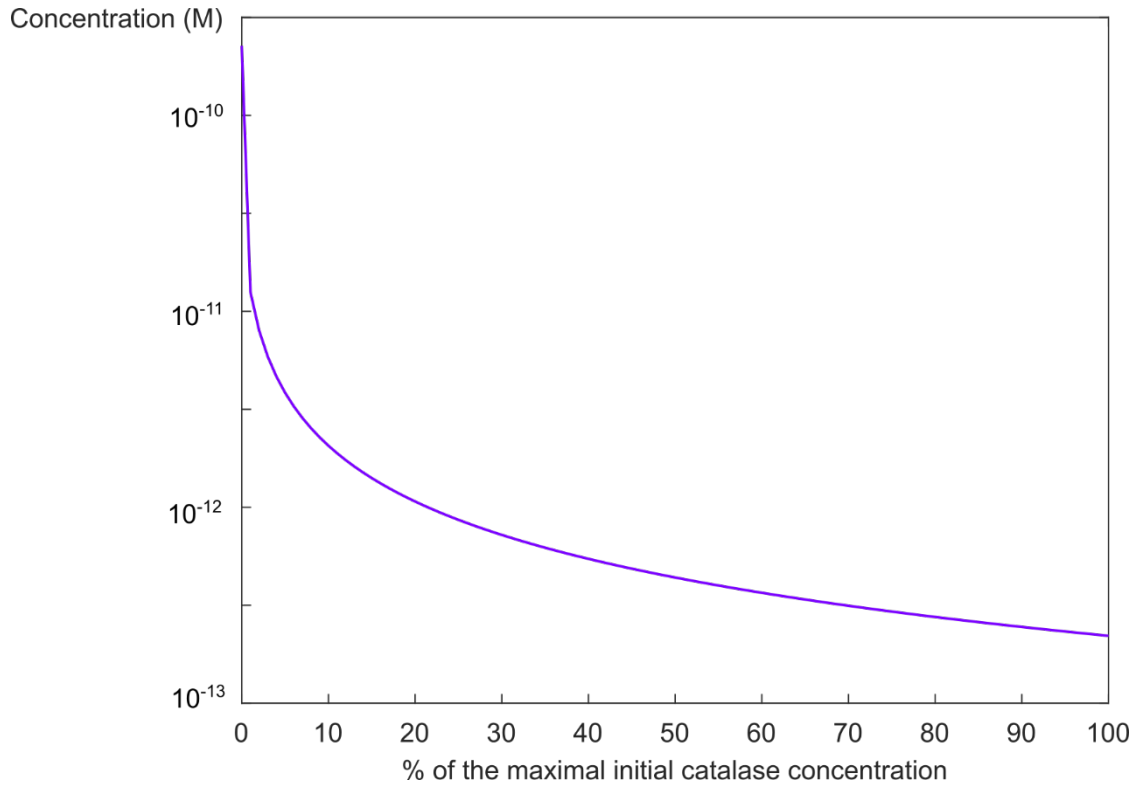


Fig 5: Hydroxyl radical concentration as a function of catalase concentration. The catalase concentration is given as % of a reference value, which in this calculation was $10^{-3} M$.

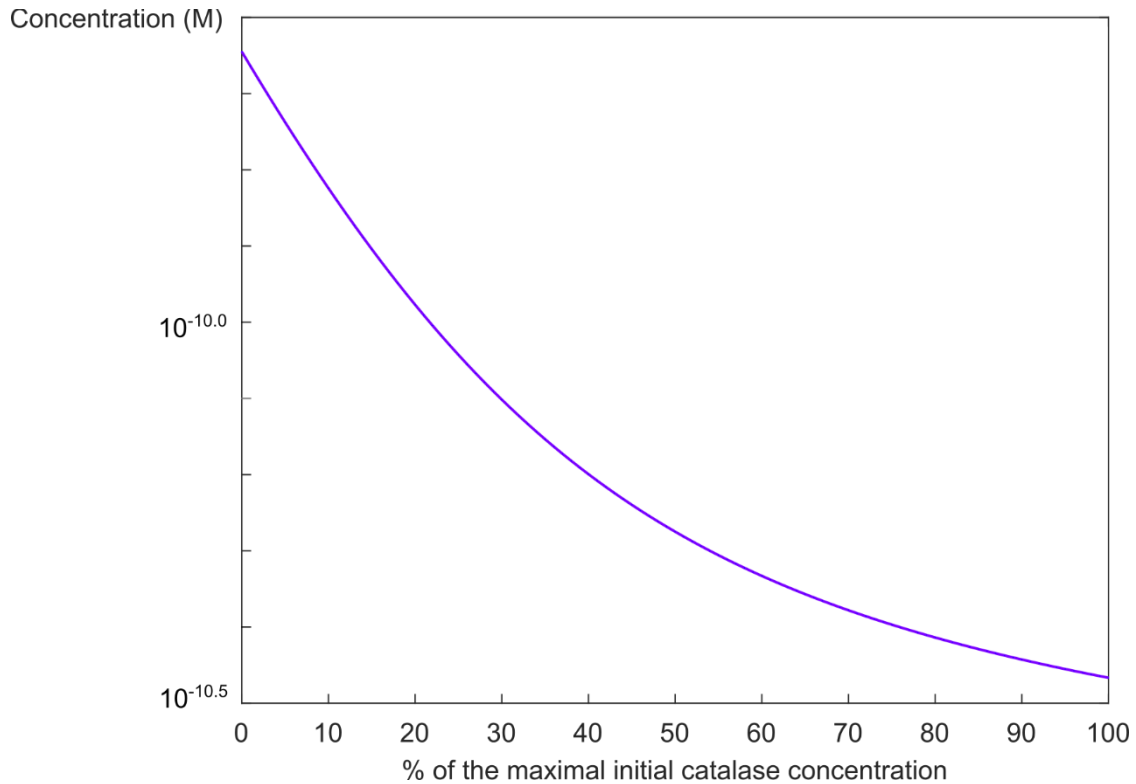


Fig 6: Hydroxyl radical concentration as a function of catalase concentration. The catalase concentration is given as % of a reference value, which in this calculation was $10^{-6} M$.

5.3 Possible interpretation of the mechanisms underlying the catalase-dependence of the generation of hydroxyl radicals

The results shown in Figs. 4-6 reveal that the relation between $\bar{x} = [CAT]_0$ and $y = [\cdot OH]_{ss}$ does not follow a simple expression. Can the key mechanisms underlying this behavior be understood? In the following we make the ansatz that the overall behavior of the nitric oxide/peroxynitrite pathway can be understood as a step-wise sequence of reactions, separated in time.

The nitric oxide/peroxynitrite pathway consists of reaction (2), (4), (7) and (8). The first reaction, reaction (2), occurs very fast and results in a $[ONOO^-]$ in the (sub) nM -regime ($[ONOO^-]_{max} = 10^{-9} M$ since $[O_2^-]_0 = 10^{-9} M$). The fate of peroxynitrite is governed by the ratio of the rates of its different pathways of consumption (here, the pathway consisting of the reverse of reaction (2) can be neglected due to a vanishing rate in comparison to the other two, see Tab. 1): decomposition by catalase (reaction (4)) and protonation into peroxy nitrous acid (reaction (7)). The ratio between the rates of these two pathways of consumption is

$$r = \frac{v_4}{v_7} = \frac{k_4 [CAT]_0}{k_7 [H^+]}$$

Inserting the values from Tabs. 1-3, it can be seen that when the two pathways occur at the same rate, i.e., $r = 1$, $[CAT]_0 \sim 6 \times 10^{-4} M$. If $r < 1$, the protonation of peroxy nitrite into peroxy nitrous acid outcompetes the decomposition by catalase. This highlights the fact that protonation of peroxy nitrite is a very crucial step in reactivating hydroxyl radical generation and hence, that the protective effect of catalase is pH-dependent in a linear manner. It suggests that in vicinity of proton pumps, where $[H^+]$ is higher than $10^{-7} M$, a higher concentration of catalase is required to protect the cancer cells from hydroxyl radical generation. It has been experimentally verified that *in vitro* the high concentration of proton pump derived protons controls the formation of peroxy nitrous acid, which leads to the generation of hydroxyl radicals at the required site of a cancer cell ³⁴. Lowering the pH could hence potentially have the same impact on the nitric oxide/peroxy nitrite pathway as inactivating catalase.

When the protonation of peroxy nitrite has occurred, the equilibrium between peroxy nitrite and peroxy nitrous acid is described by

$$\frac{[ONOOH]}{[ONOO^-][H^+]} = K_a^{-1} = 10^{pK_a} \Leftrightarrow \frac{[ONOOH]}{[ONOO^-]} = 10^{pK_a - pH}.$$

With $pK_a = 6.8$ and $pH = 7$,

$$\frac{[ONOOH]}{[ONOO^-]} = 10^{-0.2} \Leftrightarrow [ONOOH] = [ONOO^-] \times 10^{-0.2},$$

i.e., about 63% of the peroxy nitrite has been protonated.

For formation of hydroxyl radicals through reaction (8), the rate is

$$\frac{d[\cdot OH]}{dt} = k_8[ONOOH] - k_{-8}[\cdot NO_2][\cdot OH].$$

Since nitrogen dioxide and hydroxyl radicals will be formed in an equal amount and since $[\cdot OH]$ at time t will be

$$\begin{aligned} [\cdot OH]_t &= [\cdot NO_2]_t = [ONOOH]_0 - [ONOOH]_t \\ &\Leftrightarrow [ONOOH]_t = [ONOOH]_0 - [\cdot OH]_t, \end{aligned}$$

where

$$[ONOOH]_0 = [ONOO^-]_0 \times 10^{-0.2},$$

the rate of hydroxyl radicals formation takes the form

$$\frac{d[\cdot OH]_t}{dt} = k_8([ONOOH]_0 - [\cdot OH]_t) - k_{-8}([\cdot OH]_t)^2.$$

Denoting $[ONOOH]_0 = x$ and $[\cdot OH]_t = y$ and considering the steady-state of $[\cdot OH]_t$, i.e. $[\cdot OH]_t = [\cdot OH]_{ss}$,

$$k_8(x - y) - k_{-8}y^2 = 0$$

$$\Leftrightarrow y^2 + \frac{k_8y}{k_{-8}} - \frac{k_8x}{k_{-8}} = 0.$$

Expressing y in terms of x and only considering solutions where $y \geq 0$, yields

$$y = -\frac{k_8}{2k_{-8}} + \sqrt{\left(\frac{k_8}{2k_{-8}}\right)^2 + \frac{k_8 x}{k_{-8}}}.$$

For $\bar{x} = [CAT]_0 = 0 M$, $[ONOO^-]_0^{\bar{x}=0} = [ONOO^-]_{max} = 10^{-9} M$, i.e. $x = [ONOOH]_0^{\bar{x}=0} = 10^{-9.2}$ and $y \sim 2.5 * 10^{-10} M$. This is in excellent agreement with our numerical results (see previous section) and indicates that the subsequent reactions in the nitric oxide/peroxynitrite pathway can be divided into individual reactions where each of them are reaching equilibrium before the next reaction occurs when $[CAT]_0 = 0 M$.

Now, what is the situation when $[CAT]_0 \neq 0 M$?

Having derived an analytical expression that relates $[ONOOH]_0$, and hence also $[ONOO^-]_0$, to $[\cdot OH]_{ss}$, $[ONOOH]_0$ as a function of $\bar{x} = [CAT]_0$ has to be derived. Referring back to the discussion about the ratio (r) between the rates of decomposition by catalase and formation of peroxynitrous acid, respectively, this can be achieved in terms of r . If we assume that these both reactions have formed product at time $t = \tau$, where $f[ONOO^-]_0^{\bar{x} \neq 0}$ has been consumed in the formation of $[ONOOH]_0^{\bar{x} \neq 0}$ and $(1 - f)[ONOO^-]_0^{\bar{x} \neq 0}$ has been consumed in the decomposition by catalase ($0 \leq f \leq 1$), then

$$r = \frac{v_4 \tau}{v_7 \tau} = \frac{1 - f}{f},$$

i.e.,

$$f = \frac{1}{1 + r}.$$

Thus, for $\bar{x} = [CAT]_0 \neq 0$,

$$[ONOOH]_0^{\bar{x} \neq 0} = f[ONOO^-]_0^{\bar{x} \neq 0} \times 10^{-0.2} = \frac{1}{1 + r} [ONOO^-]_0^{\bar{x} \neq 0} \times 10^{-0.2}.$$

However, since there is an equilibrium between $[ONOO^-]_t$ and $[ONOOH]_t$, when peroxynitrite is decomposed by catalase, a fraction of the produced peroxynitrous acid will transform back to peroxynitrite to maintain the equilibrium. This is of course a continuous process that will start the moment that peroxynitrite starts to be decomposed by catalase, but let us assume that the process occurs in discrete cycles. In the first cycle, a fraction of the initially formed peroxynitrous acid will transform back to peroxynitrite:

$$[ONOO^-]_1^{\bar{x} \neq 0} = [ONOOH]_0^{\bar{x} \neq 0} \times 10^{0.2},$$

where the subscript denotes that the species are formed in the first cycle. A fraction of the formed peroxynitrite will form peroxynitrous acid again. The concentration is

$$[ONOOH]_1^{\bar{x} \neq 0} = \frac{1}{1 + r} [ONOO^-]_1^{\bar{x} \neq 0} \times 10^{-0.2}$$

$$= \frac{1}{1+r} [ONOOH]_0^{\bar{x} \neq 0} = \frac{1}{(1+r)^2} [ONOO^-]_0^{\bar{x} \neq 0} \times 10^{-0.2}.$$

In the same manner, the concentration of peroxy nitrous acid in the i :th cycle will be given by

$$[ONOOH]_i^{\bar{x} \neq 0} = \frac{1}{(1+r)^{i+1}} [ONOO^-]_0^{\bar{x} \neq 0} \times 10^{-0.2}.$$

If we replace $[ONOOH]_0^{\bar{x} \neq 0}$ in the derived analytical expression of $[\cdot OH]_{ss}$ to $[ONOOH]_i^{\bar{x} \neq 0}$ and try for different values of i , this can give a clue to the behavior of the relation between $\bar{x} = [CAT]_0 \neq 0$ and $y = [\cdot OH]_{ss}$. As it turns out, a similar relationship can be obtained if it is assumed that $i = i(r)$, i.e., i is dependent of r . The dependence is such that i is inversely dependent on r . It means that for a low catalase concentration, a higher number of cycles will be needed before hydroxyl radicals reaches a steady state. Since the rate of peroxy nitrite decomposition is dependent on the concentration of peroxy nitrite, it makes sense that the rate will be sufficiently high to affect the concentration of hydroxyl radicals for a higher number of cycles when a higher fraction of the peroxy nitrite is used to form peroxy nitrous acid. For high catalase concentrations, i.e., r is high, the major part of the available peroxy nitrite will be depleted already in the first cycle. Hence, the concentration of peroxy nitrite will be too low to create a significant rate of the catalase-dependent decomposition of peroxy nitrite and the hydroxyl radical concentration will reach a steady-state after a few cycles.

The conclusion of this analysis is that it might be possible to qualitatively describe the overall behavior of the nitric oxide/peroxy nitrite pathway as a step-wise sequence of reactions. In particular, a cycle-dependent pseudo-steady-state concentration of peroxy nitrous acid can be used to predict the qualitative behavior of the resulting steady-state concentration of hydroxyl radicals also when catalase is introduced in the reaction network. Even though an analytical solution of $y(\bar{x})$ probably does not exist due to the complex, nonlinear nature of the set of rate equations that govern the kinetics in the reaction network, the qualitative relationship:

$$y = -\frac{k_8}{2k_{-8}} + \sqrt{\left(\frac{k_8}{2k_{-8}}\right)^2 + \frac{k_8 [ONOOH]_i^{\bar{x} \neq 0}}{k_{-8}}},$$

where $i = i(r)$, might offer an interpretation of the key mechanisms underlying the resulting relationship between the concentration of catalase and the generation of hydroxyl radicals.

5.4 Limitations of the model and potential implications

In our mathematical model of the catalase-dependent kinetics of the reaction network of the hypochlorous acid- and the nitric oxide/peroxy nitrite pathway, we only consider the closed system as it would appear in a well-mixed reaction vessel. More about the justification of this restriction can be found in section 3.1. The analysis of the kinetics of the reaction network itself has provided us with information about the *maximal* hydroxyl radical generation from the hypochlorous acid and nitric oxide/peroxy nitrite pathways under the given conditions, and how the interaction with

catalase at various concentrations affects the resulting concentration of hydroxyl radicals. It has also revealed what concentrations of the involved ROS/RNS and enzymes are required for the hydroxyl radical generation from the hypochlorous acid- and nitric oxide/peroxynitrite pathways to represent a feasible mechanism underlying the selectivity of CAP for cancer treatment. However, in a more realistic, open system of the extracellular compartment, there are a number of effects that potentially could affect the results. These are in particular:

- The spatial dynamics of the involved species.
- The constant generation of some species (superoxide anions and nitric oxide in particular).
- The effect of interfering pathways (which in general will cause a reduction of the generation of hydroxyl radicals, because the substrates of hydroxyl radicals generation are used in the formation of other products, e.g., in the formation of singlet oxygen through interaction between hydrogen peroxide and peroxynitrite).

First, the fact that our model does not predict a generation of hydroxyl radicals from the hypochlorous acid pathway, while experiments suggest that this should be the case, indicates that both *in vitro* and *in vivo*, the spatial dynamics might play an important role. If a fraction of superoxide anions diffuses away from its site of production before reacting with nitric oxide or SOD, it could serve as a reservoir of superoxide anions for hypochlorous acid to react with. However, the production of hydroxyl radicals from the hypochlorous acid pathway might then not occur in direct vicinity to the cell membrane, which reduces the chances for hydroxyl radicals to cause lipid peroxidation (and hence, apoptosis-induction). Furthermore, other studies in similar systems predict superoxide anions to be consumed within a very narrow spatial regime from its site of production⁷⁶⁻⁷⁷. Diffusion of nitric oxide from the site of production would lead to a decreased effective concentration close to the cell membrane, thus making it more likely for superoxide anions to enter the hypochlorous acid pathway. Still, the kinetics of this reaction network predicts that $[^{\bullet}NO]$ has to decrease by many orders of magnitude and at the same time $[SOD]_0$ must be very low, in order for (a very small amount of) hydroxyl radicals to be generated from the hypochlorous acid pathway. Furthermore, the total concentration of generated hydroxyl radicals from the reaction network will be reduced in such a case.

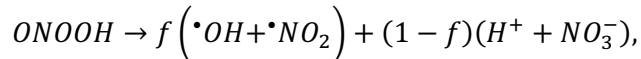
Second, it can be discussed how the results would be expected to differ if a constant generation of the species superoxide anions and nitric oxide were included in the model. Considering the time scale (about 200 times longer than the time scale relevant here) to reach a steady-state concentration of nitric oxide in a similar system⁸⁸, it can be assumed that adding such terms to the system of rate equations would not significantly change the results. If so, a constant generation of nitric oxide in the reaction network would obviously increase the fraction of superoxide anions entering the nitric oxide/peroxynitrite pathway. A constant generation of superoxide anions, on the other hand, should not change the qualitative result since also the newly generated superoxide anions would directly enter one of the two initial reactions in the reaction network - thus contributing to the formation of peroxynitrite and hydrogen peroxide - not to formation of hydroxyl radicals through reaction between hydrogen peroxide and superoxide anions. Thus, we believe the ratio of $[^{\bullet}OH]$ to $[O_2^{\bullet-}]$ would be unchanged.

Third, including any of the interfering reactions would - with one exception - only lower the total production of hydroxyl radicals from the reaction network. The exception is that FASR (which is

an apoptosis-inducing membrane-receptor) can be triggered by singlet oxygen in the absence of its genuine ligand¹⁰⁶ - a process which activates caspase-8 and enhances the NOX1 activity as well as induces NOS expression¹⁰⁷⁻¹⁰⁸. Thus, there will be an increased local generation of superoxide anions and nitric oxide. Referring back to the previous discussion, if this will significantly change the result, it will increase the peroxynitrite concentration, thus making the nitric oxide/peroxynitrite pathway stronger. Including reactions where nitric oxide is consumed is also a possible way to decrease the effective concentration of nitric oxide, which would increase the amount of superoxide anions entering the hypochlorous acid pathway. Still, as already mentioned, this causes a lower total concentration of hydroxyl radicals generated from the total reaction network.

In addition, we should also mention the effect of temperature and viscosity on the rate constants, especially since two important rate constants in the hypochlorous acid pathway (k_1 and k_6 , see section 6.1) are from studies performed at room temperature (rather than at the relevant temperature of 37°C). However, it seems unlikely that these rate constants would be increased by many orders of magnitude due to the relatively small increase in temperature. Thus, we believe that the qualitative behavior of the reaction network would not change substantially by adjusting these rate constants to 37°C. The viscosity in the extracellular compartment is probably higher than the solutions for which the included rate constant values are determined for. Since this means a slower diffusion for the reacting species, it leads to less frequent collisions and thus lower rate constants. If this effect is more noticeable for some reactions than others, it could affect the results of the model.

Regarding the nitric oxide/peroxynitrite pathway, we have not included the potential oxidation of nitric oxide by (active) catalase in this study. It has been excluded as the main effect of catalase on the nitric oxide/peroxynitrite pathway³⁴, but may be included in future models to rule out that it would have a significant effect on the concentration of nitric oxide. Two other aspects would be more important to include in the study of this pathway though. First, in biological systems the reaction between peroxynitrite and carbon dioxide¹⁰⁹⁻¹¹² is considered to be the major route of peroxynitrite decomposition since the physiological concentration of carbon dioxide is high ((1 – 3) × 10⁻² M)¹¹³. To achieve a more realistic result of the true concentration of the generated hydroxyl radicals, this reaction is hence crucial to include. Second, studies show that the formation of hydroxyl radicals from peroxynitrous acid should rather be written as



where $0 \leq f \leq 1$ is the fraction of peroxynitrous acid that undergoes radical escape. The yield of hydroxyl radicals from decomposition of peroxynitrous acid, according to the literature, varies within the range 0 – 40%¹¹⁴⁻¹²⁰, i.e. $f \leq 0.4$ whereas in this study, $f = 1$, was assumed.

Regarding the hypochlorous acid pathway and the discrepancy between our results (which predict that hydroxyl radicals is not generated from this pathway) and the experimental findings, an aspect that should be brought up in the discussion about this pathway, is that it has been shown that superoxide anions can be generated by two common components of cell culture media: HEPES buffer and (in the presence of light) riboflavin¹²¹. Thus, for *in vitro* studies in such cell culture media, some of the superoxide anions production might be attributed to the generation of the media and not by the cells themselves. In e.g. refs. ^{68, 70}, where the hypochlorous acid pathway was

studied, Eagle's Minimal Essential Medium was used for the cell cultures. Since Eagle's Minimal Essential Medium contains riboflavin and since there is nothing mentioned about the light conditions for these experiments, it cannot be ruled out that the results from these studies are affected by the production of superoxide anions by the culture medium. Another aspect regarding this pathway is that possible SOD-inactivation of CAP indicates that the hypochlorous acid pathway might be less important than the nitric oxide/peroxynitrite pathway in the context of apoptosis-induction by CAP. Indeed, since SOD shares the common feature of histidine at the active site with catalase, it is reasonable to assume that also SOD is inactivated by CAP in the same manner as catalase. It has been shown that the histidine residue of SOD is inactivated by singlet oxygen even more effectively than the histidine residue of catalase¹²²⁻¹²³. In such a case, the probability of SOD inactivation by CAP should be even higher than catalase inactivation. The immediate effect of SOD inactivation is that the rate of hydrogen peroxide formation is decreased whereas the peroxynitrite concentration is increased. Furthermore, the increased concentration of superoxide anions may cause catalase inhibition. In ref.¹⁰⁵ it is verified that inhibition of SOD increases the concentration of superoxide anions, which inhibits catalase and removes the enzymatic dismutation of superoxide anions to hydrogen peroxide, thus inhibiting the hypochlorous acid pathway. It has indeed been shown that inactivation of SOD indirectly inhibits catalase through superoxide anions dependent inhibition¹²⁴. In this study, inactivation of SOD was also found to cause a drastic decrease of hydrogen peroxide.

In ref.¹²⁵ another potential effect, contributing to hydroxyl radical induced apoptosis, is mentioned. In the case of aquaporins in the vicinity of inactivated catalase, hydrogen peroxide could be transferred from the extracellular compartment to the intracellular compartment. Here, hydrogen peroxide would cause depletion of glutathione - a process that makes the cell more sensitive to extracellular hydroxyl radicals. The resulting effect might be that the more catalase that is inactivated, the less amount of hydroxyl radicals is required to induce apoptosis. In such a case, catalase does not have to be inactivated to such a high extent that our results suggest, i.e., our results might have to be adjusted. This hypothesis is of course based on the assumption that there is a sufficient amount of hydrogen peroxide in the extracellular compartment, i.e., SOD must not have been inactivated to a large extent by singlet oxygen.

Lastly, there are some additional effects, not included in the model, that also could change the results. These are:

- The difference in catalytic action of membrane-bound enzymes as compared to enzymes that are free in solution.
- The effect of non-equilibrium on the rate constants.
- The potential enzyme inhibition by the products (or other species).
- The pH-dependence of enzyme activity.

These effects are, however, all very difficult to take into account, but may play an important role in *in vivo* systems. In summary, our model merely serves as a first step in the theoretical investigation of the catalase-dependence of the apoptosis-inducing signaling pathways suggested in ref.³⁷. Further improvement will be needed, but the model already gives important insights about necessary conditions in terms of concentrations of enzymes and ROS/RNS in order for both the hypochlorous acid- and nitric oxide/peroxynitrite pathway to be inhibited and reactivated.

6. Conclusions

In this work, we have developed and used a mathematical model to analyze and gain insights about a specific mechanism, which has been described in great detail and is proposed to explain selectivity of CAP for cancer treatment ³⁷. Explicitly, the model describes the catalase-dependent reaction kinetics of two apoptosis-inducing signaling pathways occurring in the extracellular compartment of cancer cells. By implementing this model, we investigated the possibility to reactivate the generation of hydroxyl radicals (responsible for inducing apoptosis) from the reaction network of both pathways by inactivation of catalase (which is proposed to occur upon CAP treatment). Our analysis reveals that only one of these pathways seems feasible in the context of hydroxyl radicals generation under relevant conditions, and this pathway requires very high catalase concentrations - about 1 mM - to be inhibited. In the absence of other interfering pathways and for $[SOD]_0 \lesssim 10^{-7} M$, this can indeed be assumed to be the condition of the extracellular compartment of cancer cells before CAP treatment (given that the mechanism in ref. ³⁷ is valid). In order to reactivate this pathway, about 99% of the catalase has to be inactivated.

The fact that our model fails to reproduce the reactivation of the second pathway, might indicate that further developments are needed to capture the complexity of the signaling pathways in their *in vitro* and *in vivo* context. Especially, diffusion may be of importance to decrease the effective concentration of some species close to the cell membrane. Still, the kinetics of this pathway is very unfavorable and it might also be relevant to investigate other possible mechanisms for hydroxyl radical generation from this pathway.

In spite of the limitations of the model, we believe this work contributes to a better understanding of one of the mechanisms possibly underlying the selectivity of CAP for cancer treatment. Especially, it provides insights into the necessary conditions for the mechanism to operate the way proposed and indicates that other possible mechanisms underlying the selectivity of CAP should be considered and analyzed as well.

Acknowledgments

The resources and services used in this work were provided by the VSC (Flemish Supercomputer Center), funded by the Research Foundation - Flanders (FWO) and the Flemish Government.

We thank Dr. David Graves for comments that greatly improved the manuscript.

Funding

This research did not receive any specific grant from funding agencies in the public, commercial, or not-for-profit sectors.

Appendix

We present here more detailed information about the rate equations and rate constants used, as well as how the effective radius of enzyme molecules was found.

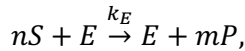
A1. Rate equations and rate constants

A1.1. General information

Reaction (3) and (5) follow Michaelis-Menten kinetics, i.e.,

$$\begin{aligned}\frac{d[P]}{dt} &= k_E [E]_0 \frac{[S]}{K_E + [S]}, \\ \frac{d[S]}{dt} &= -\frac{d[P]}{dt}, \\ \frac{d[E]}{dt} &= 0,\end{aligned}$$

where $[S]$ denotes the substrate concentration, $[P]$ denotes the product concentration, $[E]_0$ denotes the initial enzyme concentration, k_E is the catalytic constant for enzyme E and K_E is the Michaelis-Menten constant for enzyme E . For a reaction of the type



we assume the rate equation

$$-\frac{1}{n} \frac{d[S]}{dt} = \frac{1}{m} \frac{d[P]}{dt},$$

to be valid.

A1.2. Reaction (1)

In ref.¹²⁶ we found that the activity of (bovine) SOD is relatively independent of pH between 5.3 and 9.5. In ref.⁹⁷ we found that bovine SOD is catalyzing the decay of superoxide anions with a second order rate constant, $k_1 = 2.3 \times 10^9 M^{-1}s^{-1}$, at $T = 20 - 25^\circ\text{C}$ and $pH = 7.0$, where the rate of superoxide anions decay is given as

$$\frac{d[O_2^{\bullet-}]}{dt} = -k_1 [O_2^{\bullet-}][SOD].$$

The rate of formation of hydrogen peroxide should hence follow

$$\frac{d[H_2O_2]}{dt} = \frac{1}{2} k_1 [O_2^{\bullet-}][SOD].$$

In ref.⁹⁵, we found that for (bovine) SOD at $T \sim 25^\circ\text{C}$ and pH between 9.0 and 9.9, the second-order rate constant for superoxide anions decay is $k_1 = 2.4 \times 10^9 \text{ M}^{-1}\text{s}^{-1}$. The average of both values for k_1 is used in our calculations, i.e., $k_1 = 2.35 \times 10^9 \text{ M}^{-1}\text{s}^{-1}$.

A1.3. Reaction (2)

In ref.¹²⁷ the second order rate constant for the decay of superoxide anions at $T = 20 - 25^\circ\text{C}$ and $pH = 7.5$ was determined to be $k_2 = (6.7 \pm 0.9) \times 10^9 \text{ M}^{-1}\text{s}^{-1}$. The rate of the decay of superoxide anions hence is

$$\begin{aligned} \frac{d[O_2^{\bullet-}]}{dt} &= \frac{d[\bullet NO]}{dt} = -k_2[O_2^{\bullet-}][\bullet NO], \\ \Rightarrow \frac{d[ONOO^-]}{dt} &= k_2[O_2^{\bullet-}][\bullet NO]. \end{aligned}$$

In ref.¹²⁸ the rate constant for superoxide anions decay was shown to be independent of pH in the range $6.1 - 10.0$ and the rate constant was determined to be $k_2 = (4.3 \pm 0.5) \times 10^9 \text{ M}^{-1}\text{s}^{-1}$ (no information on T). In ref.¹⁰⁰, the rate constant was found to be $k_2 = 4.8 \times 10^9 \text{ M}^{-1}\text{s}^{-1}$ at $T = 25^\circ\text{C}$ and in ref.¹²⁹ the weighted average of three different experiments gave a value of $k_2 = (1.6 \pm 0.3) \times 10^{10} \text{ M}^{-1}\text{s}^{-1}$ (no information on T). In ref.⁹³, a value of $k_2 = 3.2 \times 10^{10} \text{ M}^{-1}\text{s}^{-1}$ at $T = 25^\circ\text{C}$ was reported. In ref.⁹³ it was furthermore concluded that the expected rate constant at $T = 37^\circ\text{C}$ is $k_2 = 1.7 \times 10^{10} \text{ M}^{-1}\text{s}^{-1}$. We used the latter value in our calculations since it is the only value found for the right temperature condition ($T = 37^\circ\text{C}$).

The value of the first order rate constant for the reverse reaction is $k_{-2} = 0.017 \text{ s}^{-1}$ in aqueous solutions at $T = 20^\circ\text{C}$ ¹⁰¹ as well as at $T = 25^\circ\text{C}$ ¹⁰⁰, i.e.,

$$\begin{aligned} \frac{d[ONOO^-]}{dt} &= -k_{-2}[ONOO^-] \\ \Rightarrow \frac{d[O_2^{\bullet-}]}{dt} &= \frac{d[\bullet NO]}{dt} = k_{-2}[ONOO^-]. \end{aligned}$$

A1.4. Reaction (3)

The reaction follows Michaelis-Menten kinetics (at $[H_2O_2] \leq 200 \text{ mM}$). Apparent values of K_3 and k_3 at $pH = 7.0$ and $T = 37^\circ\text{C}$ are $K_3 = 80.0 \text{ mM}$ and $k_3 = 587000.0 \text{ s}^{-1}$ ⁹¹. Note that in this reaction, it is assumed that the product is oxygen.

A1.5. Reaction (4)

The reaction was found to be catalyzed by bovine liver catalase with a (second order) rate constant, $k_4 = 1.7 \times 10^6 M^{-1}s^{-1}$ at $pH = 7.1$ and $T = 25^\circ\text{C}$ ⁷². The rate of the decay of peroxy nitrite can hence be expressed as

$$\frac{d[ONOO^-]}{dt} = -k_4[ONOO^-][CAT].$$

At $T = 37^\circ\text{C}$, the rate constant of peroxy nitrite decay was found to be 2.5 – 3 times higher than that measured at $T = 25^\circ\text{C}$. However, the authors noted that this result can only serve as an estimation due to some experimental errors. Since the difference in value anyway does not differ by many orders of magnitude, we choose to use the experimental value for $T = 25^\circ\text{C}$ in our calculations.

A1.6. Reaction (5)

The reaction follows Michaelis-Menten kinetics (with H_2O_2 as the substrate). The effect of $[Cl^-]$ and pH ($4.4 \leq pH \leq 6.2$) on the K_5 -value at $T = 37^\circ\text{C}$ for hydrogen peroxide of MPO has been studied¹³⁰ and it shows that the K_5 -values decreases with increasing $[Cl^-]$ and pH in a dose-dependent manner. In other words, as pH increases, K_5 becomes less sensitive to the concentration of chlorine anions. Hence, for $pH \sim 7$, it should be a valid assumption that K_5 changes only very little with changing $[Cl^-]$. For MPO from leukocytes at $pH = 7.2$, $T = 20^\circ\text{C}$, $[H_2O_2] = 100 \mu\text{M}$ and $[Cl^-] = 200 \text{ mM}$, $k_5 = 320 \text{ s}^{-1}$ per monomer (MPO is a homodimer, i.e., it consists of two monomers, so the effective concentration of MPO is twice the given one) and $K_5 = 30 \mu\text{M}$ during the first 100 ms ⁹² with respect to H_2O_2 . Thereafter, k_5 decreases. For lower concentrations of hydrogen peroxide ($[H_2O_2] < 50 \mu\text{M}$), k_5 is less dependent on time. Thus, for the current calculations ($[H_2O_2] \ll 50 \mu\text{M}$) it can be justified to assume that $K_5 = 30 \mu\text{M}$ is a constant in time.

A1.7. Reaction (6)

At $pH = 5.5$ and $T \sim 20^\circ\text{C}$, the decay of $O_2^{\bullet-}$ in the presence of hypochlorous acid has been determined to occur with a second order rate constant $k_6 = 7.5 \times 10^6 M^{-1}s^{-1}$ ⁹⁴, i.e.,

$$\begin{aligned} \frac{d[O_2^{\bullet-}]}{dt} &= -k_6[O_2^{\bullet-}][HOCl], \\ \Rightarrow \frac{d[\bullet OH]}{dt} &= k_6[O_2^{\bullet-}][HOCl]. \end{aligned}$$

Since no reported value of k_{-6} could be found and hydroxyl radicals is known to be a very reactive species, thus reacting with almost any other species in its surrounding, we assume that the reverse reaction is of minor importance and k_{-6} is set to 0. (A value $k_{-6} > 0$ will only reduce $[\bullet OH]$).

A1.8. Reaction (7)

The ratio of k_7 and k_{-7} is given by

$$K_a = \frac{[ONOO^-][H^+]}{[ONOOH]} = \frac{k_{-7}}{k_7} = 10^{-pK_a} M^{-1}.$$

The pK_a -value at $T = 25^\circ\text{C}$ is $6.5 - 6.8$ ^{102, 131}. To optimize the production of hydroxyl radicals, we chose $pK_a = 6.8$ in our calculations.

Diffusion-controlled second-order rate constants of protonation of a wide range of compounds are within $(0.35 - 18) \times 10^{10} M^{-1}s^{-1}$ ⁹⁶. We chose $k_7 = 10^{10} M^{-1}s^{-1}$ in our calculations.

A1.9. Reaction (8)

The rate constants in reaction (8) are $k_8 = 10^{-4} - 0.6 s^{-1}$ at $T = 25^\circ\text{C}$ ⁹⁸ and $k_{-8} = (4.5 \pm 1.0) \times 10^9 M^{-1}s^{-1}$ ($pH = 9.5$ and no information about T)⁹⁹, i.e.,

$$\frac{d[ONOOH]}{dt} = k_{-8}[\bullet NO_2][\bullet OH] - k_8[ONOOH],$$

and

$$\frac{d[\bullet OH]}{dt} = -k_{-8}[\bullet NO_2][\bullet OH] + k_8[ONOOH].$$

To find the upper limit of the hydroxyl radicals production from the nitric oxide/peroxynitrite pathway, we use the largest possible value for k_8 , i.e., $k_8 = 0.6 s^{-1}$, and the smallest possible value for k_{-8} , i.e., $k_{-8} = 3.5 \times 10^9 M^{-1}s^{-1}$.

A2. Enzyme effective radius

The effective radius of the enzymes are found by the following procedure: The pdb-file for each respective enzyme is downloaded on the protein data bank www.rcsb.org. This file is then uploaded into the protein volume calculating program “Voss Volume Voxelator” (<http://3vee.molmovdb.org/index.php>), which calculates the effective radius of the enzyme.

A2.1. Catalase

The crystal structure of catalase (*homo sapiens*) was taken from ref. ¹³². The calculations yield the effective radius equal to 25.10 Å. This yields a maximum concentration of 13.1 mM.

A2.2. SOD

The crystal structure of SOD (*homo sapiens*) was taken from ref. ¹³³. The calculations yield an effective radius of 15.70 Å. This yields a maximum concentration of 53.6 mM.

References

1. Kaushik, N. K.; Attri, P.; Kaushik, N.; Choi, E. H., A Preliminary Study of the Effect of DBD Plasma and Osmolytes on T98G Brain Cancer and HEK Non-Malignant Cells. *Molecules* **2013**, *18* (5), 4917-4928.
2. Vandamme, M.; Robert, E.; Lerondel, S.; Sarron, V.; Ries, D.; Dozias, S.; Sobilo, J.; Gosset, D.; Kieda, C.; Legrain, B.; Pouvesle, J. M.; Le Pape, A., ROS implication in a new antitumor strategy based on non-thermal plasma. *Int. J. Cancer* **2012**, *130* (9), 2185-2194.
3. Fridman, G.; Shereshevsky, A.; Jost, M. M.; Brooks, A. D.; Fridman, A.; Gutsol, A.; Vasilets, V.; Friedman, G., Floating electrode dielectric barrier discharge plasma in air promoting apoptotic behavior in melanoma skin cancer cell lines. *Plasma Chem. Plasma Process.* **2007**, *27* (2), 163-176.
4. Kim, G. C.; Kim, G. J.; Park, S. R.; Jeon, S. M.; Seo, H. J.; Iza, F.; Lee, J. K., Air plasma coupled with antibody-conjugated nanoparticles: a new weapon against cancer. *J. Phys. D-Appl. Phys.* **2009**, *42* (3), 5.
5. Lee, H. J.; Shon, C. H.; Kim, Y. S.; Kim, S.; Kim, G. C.; Kong, M. G., Degradation of adhesion molecules of G361 melanoma cells by a non-thermal atmospheric pressure microplasma. *New J. Phys.* **2009**, *11*, 13.
6. Ninomiya, K.; Ishijima, T.; Imamura, M.; Yamahara, T.; Enomoto, H.; Takahashi, K.; Tanaka, Y.; Uesugi, Y.; Shimizu, N., Evaluation of extra- and intracellular OH radical generation, cancer cell injury, and apoptosis induced by a non-thermal atmospheric-pressure plasma jet. *J. Phys. D-Appl. Phys.* **2013**, *46* (42), 8.
7. Wang, M.; Holmes, B.; Cheng, X. Q.; Zhu, W.; Keidar, M.; Zhang, L. G., Cold Atmospheric Plasma for Selectively Ablating Metastatic Breast Cancer Cells. *PLoS One* **2013**, *8* (9), 11.
8. Ishaq, M.; Evans, M. D. M.; Ostrikov, K., Atmospheric pressure gas plasma-induced colorectal cancer cell death is mediated by Nox2-ASK1 apoptosis pathways and oxidative stress is mitigated by Srx-Nrf2 anti-oxidant system. *Biochim. Biophys. Acta-Mol. Cell Res.* **2014**, *1843* (12), 2827-2837.
9. Plewa, J. M.; Yousfi, M.; Frongia, C.; Eichwald, O.; Ducommun, B.; Merbahi, N.; Lobjois, V., Low-temperature plasma-induced antiproliferative effects on multi-cellular tumor spheroids. *New J. Phys.* **2014**, *16*, 20.
10. Keidar, M.; Walk, R.; Shashurin, A.; Srinivasan, P.; Sandler, A.; Dasgupta, S.; Ravi, R.; Guerrero-Preston, R.; Trink, B., Cold plasma selectivity and the possibility of a paradigm shift in cancer therapy. *Br. J. Cancer* **2011**, *105* (9), 1295-1301.
11. Kim, J. Y.; Ballato, J.; Foy, P.; Hawkins, T.; Wei, Y. Z.; Li, J. H.; Kim, S. O., Apoptosis of lung carcinoma cells induced by a flexible optical fiber-based cold microplasma. *Biosens. Bioelectron.* **2011**, *28* (1), 333-338.
12. Ahn, H. J.; Kim, K. I.; Hoan, N. N.; Kim, C. H.; Moon, E.; Choi, K. S.; Yang, S. S.; Lee, J. S., Targeting Cancer Cells with Reactive Oxygen and Nitrogen Species Generated by Atmospheric-Pressure Air Plasma. *PLoS One* **2014**, *9* (1), 13.

13. Tan, X.; Zhao, S. S.; Lei, Q.; Lu, X. P.; He, G. Y.; Ostrikov, K., Single-Cell-Precision Microplasma-Induced Cancer Cell Apoptosis. *PLoS One* **2014**, 9 (6), 10.
14. Barekzi, N.; Laroussi, M., Dose-dependent killing of leukemia cells by low-temperature plasma. *J. Phys. D-Appl. Phys.* **2012**, 45 (42), 6.
15. Thiagarajan, M.; Anderson, H.; Gonzales, X. F., Induction of Apoptosis in Human Myeloid Leukemia Cells by Remote Exposure of Resistive Barrier Cold Plasma. *Biotechnol. Bioeng.* **2014**, 111 (3), 565-574.
16. Metelmann, H. R.; Nedrelow, D. S.; Seebauer, C.; Schuster, M.; von Woedtke, T.; Weltmann, K. D.; Kindler, S.; Metelmann, P. H.; Finkelstein, S. E.; Von Hoff, D. D.; Podmelle, F., Head and neck cancer treatment and physical plasma. *Clin. Plasma Med.* **2015**, 3 (1), 17-23.
17. Metelmann, H. R.; Seebauer, C.; Miller, V.; Fridman, A.; Bauer, G.; Graves, D. B.; Pouvesle, J. M.; Rutkowski, R.; Schuster, M.; Bekeschus, S.; Wende, K.; Masur, K.; Hasse, S.; Gerling, T.; Hori, M.; Tanaka, H.; Choi, E. H.; Weltmann, K. D.; Metelmann, P. H.; Von Hoff, D. D.; von Woedtke, T., Clinical experience with cold plasma in the treatment of locally advanced head and neck cancer. *Clin. Plasma Med.* **2018**, 9, 6-13.
18. Schuster, M.; Seebauer, C.; Rutkowski, R.; Hauschild, A.; Podmelle, F.; Metelmann, C.; Metelmann, B.; von Woedtke, T.; Hasse, S.; Weltmann, K. D.; Metelmann, H. R., Visible tumor surface response to physical plasma and apoptotic cell kill in head and neck cancer. *J. Crano-MaxilloFac. Surg.* **2016**, 44 (9), 1445-1452.
19. Adachi, T.; Nonomura, S.; Horiba, M.; Hirayama, T.; Kamiya, T.; Nagasawa, H.; Hara, H., Iron stimulates plasma-activated medium-induced A549 cell injury. *Sci Rep* **2016**, 6, 12.
20. Guerrero-Preston, R.; Ogawa, T.; Uemura, M.; Shumulinsky, G.; Valle, B. L.; Pirini, F.; Ravi, R.; Sidransky, D.; Keidar, M.; Trink, B., Cold atmospheric plasma treatment selectively targets head and neck squamous cell carcinoma cells. *Int. J. Mol. Med.* **2014**, 34 (4), 941-946.
21. Iseki, S.; Nakamura, K.; Hayashi, M.; Tanaka, H.; Kondo, H.; Kajiyama, H.; Kano, H.; Kikkawa, F.; Hori, M., Selective killing of ovarian cancer cells through induction of apoptosis by nonequilibrium atmospheric pressure plasma. *Appl. Phys. Lett.* **2012**, 100 (11), 4.
22. Ishaq, M.; Kumar, S.; Varinli, H.; Han, Z. J.; Rider, A. E.; Evans, M. D. M.; Murphy, A. B.; Ostrikov, K., Atmospheric gas plasma-induced ROS production activates TNF-ASK1 pathway for the induction of melanoma cancer cell apoptosis. *Mol. Biol. Cell* **2014**, 25 (9), 1523-1531.
23. Kaushik, N. K.; Kaushik, N.; Park, D.; Choi, E. H., Altered Antioxidant System Stimulates Dielectric Barrier Discharge Plasma-Induced Cell Death for Solid Tumor Cell Treatment. *PLoS One* **2014**, 9 (7), 11.
24. Kim, S. J.; Chung, T. H., Cold atmospheric plasma jet-generated RONS and their selective effects on normal and carcinoma cells. *Sci Rep* **2016**, 6, 14.
25. Kumar, N.; Park, J. H.; Jeon, S. N.; Park, B. S.; Choi, E. H.; Attri, P., The action of microsecond-pulsed plasma-activated media on the inactivation of human lung cancer cells. *J. Phys. D-Appl. Phys.* **2016**, 49 (11), 9.
26. Kurake, N.; Tanaka, H.; Ishikawa, K.; Kondo, T.; Sekine, M.; Nakamura, K.; Kajiyama, H.; Kikkawa, F.; Mizuno, M.; Hori, M., Cell survival of glioblastoma grown in medium containing hydrogen peroxide and/or nitrite, or in plasma-activated medium. *Arch. Biochem. Biophys.* **2016**, 605, 102-108.
27. Siu, A.; Volotskova, O.; Cheng, X. Q.; Khalsa, S. S.; Bian, K.; Murad, F.; Keidar, M.; Sherman, J. H., Differential Effects of Cold Atmospheric Plasma in the Treatment of Malignant Glioma. *PLoS One* **2015**, 10 (6), 14.
28. Utsumi, F.; Kajiyama, H.; Nakamura, K.; Tanaka, H.; Hori, M.; Kikkawa, F., Selective cytotoxicity of indirect nonequilibrium atmospheric pressure plasma against ovarian clear-cell carcinoma. *SpringerPlus* **2014**, 3, 9.

29. Biscop, E.; Lin, A.; Van Boxem, W.; Van Loenhout, J.; De Backer, J.; Deben, C.; Dewilde, S.; Smits, E.; Bogaerts, A., Influence of Cell Type and Culture Medium on Determining Cancer Selectivity of Cold Atmospheric Plasma Treatment. *cancers* **2019**, *11* (9), 1287-1301.

30. Ahn, H. J.; Kim, K. I.; Kim, G.; Moon, E.; Yang, S. S.; Lee, J. S., Atmospheric-Pressure Plasma Jet Induces Apoptosis Involving Mitochondria via Generation of Free Radicals. *PLoS One* **2011**, *6* (11), 7.

31. Arjunan, K. P.; Friedman, G.; Friedman, A.; Clyne, A. M., Non-thermal dielectric barrier discharge plasma induces angiogenesis through reactive oxygen species. *J. R. Soc. Interface* **2012**, *9* (66), 147-157.

32. Yan, X.; Xiong, Z. L.; Zou, F.; Zhao, S. S.; Lu, X. P.; Yang, G. X.; He, G. Y.; Ostrikov, K., Plasma-Induced Death of HepG2 Cancer Cells: Intracellular Effects of Reactive Species. *Plasma Process. Polym.* **2012**, *9* (1), 59-66.

33. Barekzi, N.; Laroussi, M., Effects of Low Temperature Plasmas on Cancer Cells. *Plasma Process. Polym.* **2013**, *10* (12), 1039-1050.

34. Bauer, G., Increasing the endogenous NO level causes catalase inactivation and reactivation of intercellular apoptosis signaling specifically in tumor cells. *Redox Biol.* **2015**, *6*, 353-371.

35. Bauer, G., The Antitumor Effect of Singlet Oxygen. *Anticancer Res.* **2016**, *36* (11), 5649-5663.

36. Bauer, G., Central Signaling Elements of Intercellular Reactive Oxygen/Nitrogen Species-dependent Induction of Apoptosis in Malignant Cells. *Anticancer Res.* **2017**, *37* (2), 499-513.

37. Bauer, G.; Graves, D. B., Mechanisms of Selective Antitumor Action of Cold Atmospheric Plasma-Derived Reactive Oxygen and Nitrogen Species. *Plasma Process. Polym.* **2016**, *13* (12), 1157-1178.

38. Gay-Mimbrera, J.; Garcia, M. C.; Isla-Tejera, B.; Rodero-Serrano, A.; Garcia-Nieto, A. V.; Ruano, J., Clinical and Biological Principles of Cold Atmospheric Plasma Application in Skin Cancer. *Adv. Ther.* **2016**, *33* (6), 894-909.

39. Keidar, M., Plasma for cancer treatment. *Plasma Sources Sci. Technol.* **2015**, *24* (3), 20.

40. Keidar, M.; Shashurin, A.; Volotskova, O.; Stepp, M. A.; Srinivasan, P.; Sandler, A.; Trink, B., Cold atmospheric plasma in cancer therapy. *Phys. Plasmas* **2013**, *20* (5), 8.

41. Ratovitski, E. A.; Cheng, X. Q.; Yan, D. Y.; Sherman, J. H.; Canady, J.; Trink, B.; Keidar, M., Anti-Cancer Therapies of 21st Century: Novel Approach to Treat Human Cancers Using Cold Atmospheric Plasma. *Plasma Process. Polym.* **2014**, *11* (12), 1128-1137.

42. Riethmuller, M.; Burger, N.; Bauer, G., Singlet oxygen treatment of tumor cells triggers extracellular singlet oxygen generation, catalase inactivation and reactivation of intercellular apoptosis-inducing signaling. *Redox Biol.* **2015**, *6*, 157-168.

43. Joh, H. M.; Kim, S. J.; Chung, T. H.; Leem, S. H., Reactive oxygen species-related plasma effects on the apoptosis of human bladder cancer cells in atmospheric pressure pulsed plasma jets. *Appl. Phys. Lett.* **2012**, *101* (5), 5.

44. Kim, C. H.; Bahn, J. H.; Lee, S. H.; Kim, G. Y.; Jun, S. I.; Lee, K.; Baek, S. J., Induction of cell growth arrest by atmospheric non-thermal plasma in colorectal cancer cells. *J. Biotechnol.* **2010**, *150* (4), 530-538.

45. Kim, S. J.; Chung, T. H.; Bae, S. H.; Leem, S. H., Induction of apoptosis in human breast cancer cells by a pulsed atmospheric pressure plasma jet. *Appl. Phys. Lett.* **2010**, *97* (2), 3.

46. Yan, D. Y.; Sherman, J. H.; Keidar, M., Cold atmospheric plasma, a novel promising anti-cancer treatment modality. *Oncotarget* **2017**, *8* (9), 15977-15995.

47. Bauer, G.; Sersenová, D.; Graves, D. B.; Machala, Z., Cold Atmospheric Plasma and Plasma-Activated Medium Trigger RONS-Based Tumor Cell Apoptosis. *Sci Rep* **2019**, *9* (1), 14210.

48. Bauer, G.; Sersenová, D.; Graves, D. B.; Machala, Z., Dynamics of Singlet Oxygen-Triggered, RONS-Based Apoptosis Induction after Treatment of Tumor Cells with Cold Atmospheric Plasma or Plasma-Activated Medium. *Sci Rep* **2019**, *9* (1), 13931.

49. Du, J.; Liu, J.; Smith, B. J.; Tsao, M. S.; Cullen, J. J., Role of Rac1-dependent NADPH oxidase in the growth of pancreatic cancer. *Cancer Gene Ther.* **2011**, *18* (2), 135-143.

50. Irani, K.; Goldschmidt-Clermont, P. J., Ras, superoxide and signal transduction. *Biochem. Pharmacol.* **1998**, *55* (9), 1339-1346.

51. Irani, K.; Xia, Y.; Zweier, J. L.; Sollott, S. J.; Der, C. J.; Fearon, E. R.; Sundaresan, M.; Finkel, T.; GoldschmidtClermont, P. J., Mitogenic signaling mediated by oxidants in ras-transformed fibroblasts. *Science* **1997**, *275* (5306), 1649-1652.

52. Kamata, T., Roles of Nox1 and other Nox isoforms in cancer development. *Cancer Sci.* **2009**, *100* (8), 1382-1388.

53. Lambeth, J. D., Nox enzymes, ROS, and chronic disease: An example of antagonistic pleiotropy. *Free Radic. Biol. Med.* **2007**, *43* (3), 332-347.

54. Laurent, E.; McCoy, J. W.; Macina, R. A.; Liu, W. H.; Cheng, G. J.; Robine, S.; Papkoff, J.; Lambeth, J. D., Nox1 is over-expressed in human colon cancers and correlates with activating mutations in K-Ras. *Int. J. Cancer* **2008**, *123* (1), 100-107.

55. Ma, Q.; Cavallin, L. E.; Yan, B.; Zhu, S. K.; Duran, E. M.; Wang, H. L.; Hale, L. P.; Dong, C. M.; Ceserman, E.; Mesri, E. A.; Goldschmidt-Clermont, P. J., Antitumorigenesis of antioxidants in a transgenic Rac1 model of Kaposi's sarcoma. *Proc. Natl. Acad. Sci. U. S. A.* **2009**, *106* (21), 8683-8688.

56. Mitsushita, J.; Lambeth, J. D.; Kamata, T., The superoxide-generating oxidase Nox1 is functionally required for Ras oncogene transformation. *Cancer Res.* **2004**, *64* (10), 3580-3585.

57. Suh, Y. A.; Arnold, R. S.; Lassegue, B.; Shi, J.; Xu, X. X.; Sorescu, D.; Chung, A. B.; Griendlung, K. K.; Lambeth, J. D., Cell transformation by the superoxide-generating oxidase Mox1. *Nature* **1999**, *401* (6748), 79-82.

58. Tominaga, K.; Kawahara, T.; Sano, T.; Toida, K.; Kuwano, Y.; Sasaki, H.; Kawai, T.; Teshima-Kondo, S.; Rokutan, K., Evidence for cancer-associated expression of NADPH oxidase 1 (Nox1)-based oxidase system in the human stomach. *Free Radic. Biol. Med.* **2007**, *43* (12), 1627-1638.

59. Weinberg, F.; Chandel, N. S., Reactive oxygen species-dependent signaling regulates cancer. *Cell. Mol. Life Sci.* **2009**, *66* (23), 3663-3673.

60. Yang, J. Q.; Li, S. J.; Domann, F. E.; Buettner, G. R.; Oberley, L. W., Superoxide generation in v-Haras-transduced human keratinocyte HaCaT cells. *Mol. Carcinog.* **1999**, *26* (3), 180-188.

61. Szatrowski, T. P.; Nathan, C. F., PRODUCTION OF LARGE AMOUNTS OF HYDROGEN-PEROXIDE BY HUMAN TUMOR-CELLS. *Cancer Res.* **1991**, *51* (3), 794-798.

62. Turner, C. P.; Toye, A. M.; Jones, O. T. G., Keratinocyte superoxide generation. *Free Radic. Biol. Med.* **1998**, *24* (3), 401-407.

63. Bauer, G., Tumor Cell-protective Catalase as a Novel Target for Rational Therapeutic Approaches Based on Specific Intercellular ROS Signaling. *Anticancer Res.* **2012**, *32* (7), 2599-2624.

64. Bauer, G., Targeting Extracellular ROS Signaling of Tumor Cells. *Anticancer Res.* **2014**, *34* (4), 1467-1482.

65. Bechtel, W.; Bauer, G., Catalase Protects Tumor Cells from Apoptosis Induction by Intercellular ROS Signaling. *Anticancer Res.* **2009**, *29* (11), 4541-4557.

66. Bohm, B.; Heinzelmann, S.; Motz, M.; Bauer, G., Extracellular localization of catalase is associated with the transformed state of malignant cells. *Biol. Chem.* **2015**, *396* (12), 1339-1356.

67. Heinzelmann, S.; Bauer, G., Multiple protective functions of catalase against intercellular apoptosis-inducing ROS signaling of human tumor cells. *Biol. Chem.* **2010**, *391* (6), 675-693.

68. Engelmann, I.; Dormann, S.; Saran, M.; Bauer, G., Transformed target cell-derived superoxide anions drive apoptosis induction by myeloperoxidase. *Redox Rep.* **2000**, *5* (4), 207-214.

69. Heigold, S.; Sers, C.; Bechtel, W.; Ivanovas, B.; Schafer, R.; Bauer, G., Nitric oxide mediates apoptosis induction selectively in transformed fibroblasts compared to nontransformed fibroblasts. *Carcinogenesis* **2002**, *23* (6), 929-941.

70. Herdener, M.; Heigold, S.; Saran, M.; Bauer, G., Target cell-derived superoxide anions cause efficiency and selectivity of intercellular induction of apoptosis. *Free Radic. Biol. Med.* **2000**, 29 (12), 1260-1271.

71. Brunelli, L.; Yermilov, V.; Beckman, J., Modulation of catalase peroxidatic and catalatic activity by nitric oxide. *Free Radic. Biol. Med.* **2001**, 30 (7), 709-714.

72. Gebicka, L.; Didik, J., Catalytic scavenging of peroxynitrite by catalase. *J. Inorg. Biochem.* **2009**, 103 (10), 1375-1379.

73. Hirst, A. M.; Simms, M. S.; Mann, V. M.; Maitland, N. J.; O'Connell, D.; Frame, F. M., Low-temperature plasma treatment induces DNA damage leading to necrotic cell death in primary prostate epithelial cells. *Br. J. Cancer* **2015**, 112 (9), 1536-1545.

74. Adimora, N. J.; Jones, D. P.; Kemp, M. L., A Model of Redox Kinetics Implicates the Thiol Proteome in Cellular Hydrogen Peroxide Responses. *Antioxid. Redox Signal.* **2010**, 13 (6), 731-743.

75. Benfeitas, R.; Selvaggio, G.; Antunes, F.; Coelho, P.; Salvador, A., Hydrogen peroxide metabolism and sensing in human erythrocytes: A validated kinetic model and reappraisal of the role of peroxiredoxin II. *Free Radic. Biol. Med.* **2014**, 74, 35-49.

76. Chen, B.; Deen, W. M., Analysis of the effects of cell spacing and liquid depth on nitric oxide and its oxidation products in cell cultures. *Chem. Res. Toxicol.* **2001**, 14 (1), 135-147.

77. Chen, B.; Deen, W. M., Effect of liquid depth on the synthesis and oxidation of nitric oxide in macrophage cultures. *Chem. Res. Toxicol.* **2002**, 15 (4), 490-496.

78. Chen, B.; Keshive, M.; Deen, W. M., Diffusion and reaction of nitric oxide in suspension cell cultures. *Biophys. J.* **1998**, 75 (2), 745-754.

79. Chin, M. P.; Deen, W. M., Prediction of nitric oxide concentrations in melanomas. *Nitric Oxide-Biol. Chem.* **2010**, 23 (4), 319-326.

80. Chin, M. P.; Schauer, D. B.; Deen, W. M., Nitric Oxide, Oxygen, and Superoxide Formation and Consumption in Macrophages and Colonic Epithelial Cells. *Chem. Res. Toxicol.* **2010**, 23 (4), 778-787.

81. Hu, T. M.; Hayton, W. L.; Mallery, S. R., Kinetic modeling of nitric-oxide-associated reaction network. *Pharm. Res.* **2006**, 23 (8), 1702-1711.

82. Komalapriya, C.; Kaloriti, D.; Tillmann, A. T.; Yin, Z. K.; Herrero-de-Dios, C.; Jacobsen, M. D.; Belmonte, R. C.; Cameron, G.; Haynes, K.; Grebogi, C.; de Moura, A. P. S.; Gow, N. A. R.; Thiel, M.; Quinn, J.; Brown, A. J. P.; Romano, M. C., Integrative Model of Oxidative Stress Adaptation in the Fungal Pathogen *Candida albicans*. *PLoS One* **2015**, 10 (9), 32.

83. Lim, C. H.; Dedon, P. C.; Deen, W. A., Kinetic Analysis of Intracellular Concentrations of Reactive Nitrogen Species. *Chem. Res. Toxicol.* **2008**, 21 (11), 2134-2147.

84. Lim, J. B.; Huang, B. K.; Deen, W. M.; Sikes, H. D., Analysis of the lifetime and spatial localization of hydrogen peroxide generated in the cytosol using a reduced kinetic model. *Free Radic. Biol. Med.* **2015**, 89, 47-53.

85. Nalwaya, N.; Deen, W. M., Analysis of the effects of nitric oxide and oxygen on nitric oxide production by macrophages. *J. Theor. Biol.* **2004**, 226 (4), 409-419.

86. Nalwaya, N.; Deen, W. M., Peroxynitrite exposure of cells cocultured with macrophages. *Ann. Biomed. Eng.* **2004**, 32 (5), 664-676.

87. Lewis, R. S.; Tamir, S.; Tannenbaum, S. R.; Deen, W. M., KINETIC-ANALYSIS OF THE FATE OF NITRIC-OXIDE SYNTHESIZED BY MACROPHAGES IN-VITRO. *J. Biol. Chem.* **1995**, 270 (49), 29350-29355.

88. Nalwaya, N.; Deen, W. M., Nitric oxide, oxygen, and superoxide formation and consumption in macrophage cultures. *Chem. Res. Toxicol.* **2005**, 18 (3), 486-493.

89. Attri, P.; Kim, Y. H.; Park, D. H.; Park, J. H.; Hong, Y. J.; Uhm, H. S.; Kim, K. N.; Fridman, A.; Choi, E. H., Generation mechanism of hydroxyl radical species and its lifetime prediction during the plasma-initiated ultraviolet (UV) photolysis. *Sci Rep* **2015**, 5, 8.

90. Kim, Y. H.; Hong, Y. J.; Baik, K. Y.; Kwon, G. C.; Choi, J. J.; Cho, G. S.; Uhm, H. S.; Kim, D. Y.; Choi, E. H., Measurement of Reactive Hydroxyl Radical Species Inside the Biosolutions During Non-thermal Atmospheric Pressure Plasma Jet Bombardment onto the Solution. *Plasma Chem. Plasma Process.* **2014**, 34 (3), 457-472.

91. Switala, J.; Loewen, P. C., Diversity of properties among catalases. *Arch. Biochem. Biophys.* **2002**, 401 (2), 145-154.

92. Zuurbier, K. W. M.; Bakkenist, A. R. J.; Wever, R.; Muijsers, A. O., THE CHLORINATING ACTIVITY OF HUMAN MYELOPEROXIDASE - HIGH INITIAL ACTIVITY AT NEUTRAL PH VALUE AND ACTIVATION BY ELECTRON-DONORS. *Biochimica Et Biophysica Acta* **1990**, 1037 (2), 140-146.

93. Botti, H.; Moller, M. N.; Steinmann, D.; Nauser, T.; Koppenol, W. H.; Denicola, A.; Radi, R., Distance-Dependent Diffusion-Controlled Reaction of (NO)-N-center dot and O-2(center dot-) at Chemical Equilibrium with ONOO. *J. Phys. Chem. B* **2010**, 114 (49), 16584-16593.

94. Candeias, L. P.; Patel, K. B.; Stratford, M. R. L.; Wardman, P., FREE HYDROXYL RADICALS ARE FORMED ON REACTION BETWEEN THE NEUTROPHIL-DERIVED SPECIES SUPEROXIDE ANION AND HYPOCHLOROUS ACID. *FEBS Lett.* **1993**, 333 (1-2), 151-153.

95. Fielden, E. M.; Roberts, P. B.; Bray, R. C.; Lowe, D. J.; Mautner, G. N.; Rotilio, G.; Calabrese, L., MECHANISM OF ACTION OF SUPEROXIDE-DISMUTASE FROM PULSE-RADIOLYSIS AND ELECTRON-PARAMAGNETIC RESONANCE - EVIDENCE THAT ONLY HALF ACTIVE-SITES FUNCTION IN CATALYSIS. *Biochem. J.* **1974**, 139 (1), 49-60.

96. Gutman, M.; Nachliel, E., THE DYNAMIC ASPECTS OF PROTON-TRANSFER PROCESSES. *Biochimica Et Biophysica Acta* **1990**, 1015 (3), 391-414.

97. Klug, D.; Fridovich, I.; Rabani, J., DIRECT DEMONSTRATION OF CATALYTIC ACTION OF SUPEROXIDE DISMUTASE THROUGH USE OF PULSE RADIOLYSIS. *J. Biol. Chem.* **1972**, 247 (15), 4839-+.

98. Koppenol, W. H.; Kissner, R., Can O = NOOH undergo homolysis? *Chem. Res. Toxicol.* **1998**, 11 (2), 87-90.

99. Logager, T.; Sehested, K., FORMATION AND DECAY OF PEROXYNITROUS ACID - A PULSE-RADIOLYSIS STUDY. *J. Phys. Chem.* **1993**, 97 (25), 6664-6669.

100. Lymar, S. V.; Poskrebyshev, G. A., Rate of ON-OO- bond homolysis and the Gibbs energy of formation of peroxy nitrite. *J. Phys. Chem. A* **2003**, 107 (39), 7991-7996.

101. Merenyi, G.; Lind, J., Free radical formation in the peroxy nitrous acid (ONOOH) peroxy nitrite (ONOO-) system. *Chem. Res. Toxicol.* **1998**, 11 (4), 243-246.

102. Pryor, W. A.; Squadrito, G. L., THE CHEMISTRY OF PEROXYNITRITE - A PRODUCT FROM THE REACTION OF NITRIC-OXIDE WITH SUPEROXIDE. *Am. J. Physiol.-Lung Cell. Mol. Physiol.* **1995**, 268 (5), L699-L722.

103. Malinski, T.; Taha, Z.; Grunfeld, S.; Patton, S.; Kapturczak, M.; Tomboulian, P., DIFFUSION OF NITRIC-OXIDE IN THE AORTA WALL MONITORED IN-SITU BY PORPHYRINIC MICROSENSORS. *Biochem. Biophys. Res. Commun.* **1993**, 193 (3), 1076-1082.

104. Furtmuller, P. G.; Burner, U.; Regelsberger, G.; Obinger, C., Spectral and kinetic studies on the formation of eosinophil peroxidase compound I and its reaction with halides and thiocyanate. *Biochemistry* **2000**, 39 (50), 15578-15584.

105. Bauer, G., siRNA-based Analysis of the Abrogation of the Protective Function of Membrane-associated Catalase of Tumor Cells. *Anticancer Res.* **2017**, 37 (2), 567-581.

106. Zhuang, S. G.; Demirs, J. T.; Kochevar, I. E., Protein kinase C inhibits singlet oxygen-induced apoptosis by decreasing caspase-8 activation. *Oncogene* **2001**, 20 (46), 6764-6776.

107. Selleri, C.; Sato, T.; Raiola, A. M.; Rotoli, B.; Young, N. S.; Maciejewski, J. P., Induction of nitric oxide synthase is involved in the mechanism of Fas-mediated apoptosis in haemopoietic cells. *Br. J. Haematol.* **1997**, 99 (3), 481-489.

108. Suzuki, Y.; Ono, Y.; Hirabayashi, Y., Rapid and specific reactive oxygen species generation via NADPH oxidase activation during Fas-mediated apoptosis. *FEBS Lett.* **1998**, 425 (2), 209-212.

109. Augusto, O.; Bonini, M. G.; Amanso, A. M.; Linares, E.; Santos, C. C. X.; De Menezes, S. L., Nitrogen dioxide and carbonate radical anion: Two emerging radicals in biology. *Free Radic. Biol. Med.* **2002**, 32 (9), 841-859.

110. Denicola, A.; Freeman, B. A.; Trujillo, M.; Radi, R., Peroxynitrite reaction with carbon dioxide/bicarbonate: Kinetics and influence on peroxynitrite-mediated oxidations. *Arch. Biochem. Biophys.* **1996**, 333 (1), 49-58.

111. Espey, M. G.; Miranda, K. M.; Thomas, D. D.; Xavier, S.; Citrin, D.; Vitek, M. P.; Wink, D. A., A chemical perspective on the interplay between NO, reactive oxygen species, and reactive nitrogen oxide species. In *Nitric Oxide: Novel Actions, Deleterious Effects and Clinical Potential*, Chiueh, C. C.; Hong, J. S.; Leong, S. K., Eds. New York Acad Sciences: New York, 2002; Vol. 962, pp 195-206.

112. Squadrito, G. L.; Pryor, W. A., Oxidative chemistry of nitric oxide: The roles of superoxide, peroxynitrite, and carbon dioxide. *Free Radic. Biol. Med.* **1998**, 25 (4-5), 392-403.

113. Zhu, L.; Gunn, C.; Beckman, J. S., BACTERICIDAL ACTIVITY OF PEROXYNITRITE. *Arch. Biochem. Biophys.* **1992**, 298 (2), 452-457.

114. Coddington, J. W.; Hurst, J. K.; Lymar, S. V., Hydroxyl radical formation during peroxynitrous acid decomposition. *J. Am. Chem. Soc.* **1999**, 121 (11), 2438-2443.

115. Crow, J. P.; Spruell, C.; Chen, J.; Gunn, C.; Ischiropoulos, H.; Tsai, M.; Smith, C. D.; Radi, R.; Koppenol, W. H.; Beckman, J. S., ON THE PH-DEPENDENT YIELD OF HYDROXYL RADICAL PRODUCTS FROM PEROXYNITRITE. *Free Radic. Biol. Med.* **1994**, 16 (3), 331-338.

116. Gerasimov, O. V.; Lymar, S. V., The yield of hydroxyl radical from the decomposition of peroxynitrous acid. *Inorg. Chem.* **1999**, 38 (19), 4317-4321.

117. Kirsch, M.; Korth, H. G.; Wensing, A.; Sustmann, R.; de Groot, H., Product formation and kinetic simulations in the pH range 1-14 account for a free-radical mechanism of peroxynitrite decomposition. *Arch. Biochem. Biophys.* **2003**, 418 (2), 133-150.

118. Kissner, R.; Nauser, T.; Kurz, C.; Koppenol, W. H., Peroxynitrous acid - Where is the hydroxyl radical? *IUBMB Life* **2003**, 55 (10-11), 567-572.

119. Richeson, C. E.; Mulder, P.; Bowry, V. W.; Ingold, K. U., The complex chemistry of peroxynitrite decomposition: New insights. *J. Am. Chem. Soc.* **1998**, 120 (29), 7211-7219.

120. Yang, G.; Candy, T. E. G.; Boaro, M.; Wilkin, H. E.; Jones, P.; Nazhat, N. B.; Saadallanazhat, R. A.; Blake, D. R., FREE-RADICAL YIELDS FROM THE HOMOLYSIS OF PEROXYNITROUS ACID. *Free Radic. Biol. Med.* **1992**, 12 (4), 327-330.

121. Keynes, R. G.; Griffiths, C.; Garthwaite, J., Superoxide-dependent consumption of nitric oxide in biological media may confound in vitro experiments. *Biochem. J.* **2003**, 369, 399-406.

122. Escobar, J. A.; Rubio, M. A.; Lissi, E. A., SOD and catalase inactivation by singlet oxygen and peroxy radicals. *Free Radic. Biol. Med.* **1996**, 20 (3), 285-290.

123. Kim, S. Y.; Kwon, O. J.; Park, J. W., Inactivation of catalase and superoxide dismutase by singlet oxygen derived from photoactivated dye. *Biochimie* **2001**, 83 (5), 437-444.

124. Bauer, G.; Motz, M., The Antitumor Effect of Single-domain Antibodies Directed Towards Membrane-associated Catalase and Superoxide Dismutase. *Anticancer Res.* **2016**, 36 (11), 5945-5956.

125. Bauer, G., Signal Amplification by Tumor Cells: Clue to the Understanding of the Antitumor Effects of Cold Atmospheric Plasma and Plasma-Activated Medium. *IEEE Trans. Radiat. Plasma Med. Sci.* **2018**, 2 (2), 87-98.

126. Rotilio, G.; Fielden, E. M.; Bray, R. C., PULSE RADIOLYSIS STUDY OF SUPEROXIDE DISMUTASE. *Biochimica Et Biophysica Acta* **1972**, 268 (2), 605-&.

127. Huie, R. E.; Padmaja, S., THE REACTION OF NO WITH SUPEROXIDE. *Free Radic. Res. Commun.* **1993**, 18 (4), 195-199.

128. Goldstein, S.; Czapski, G., THE REACTION OF NO-CENTER-DOT WITH O-2(CENTER-DOT-) AND HO2-CENTER-DOT - A PULSE-RADIOLYSIS STUDY. *Free Radic. Biol. Med.* **1995**, *19* (4), 505-510.

129. Nauser, T.; Koppenol, W. H., The rate constant of the reaction of superoxide with nitrogen monoxide: Approaching the diffusion limit. *J. Phys. Chem. A* **2002**, *106* (16), 4084-4086.

130. Andrews, P. C.; Parnes, C.; Krinsky, N. I., COMPARISON OF MYELOPEROXIDASE AND HEMI-MYELOPEROXIDASE WITH RESPECT TO CATALYSIS, REGULATION, AND BACTERICIDAL ACTIVITY. *Arch. Biochem. Biophys.* **1984**, *228* (2), 439-442.

131. Kissner, R.; Nauser, T.; Bugnon, P.; Lye, P. G.; Koppenol, W. H., Formation and properties of peroxynitrite as studied by laser flash photolysis, high-pressure stopped-flow technique, and pulse radiolysis. *Chem. Res. Toxicol.* **1997**, *10* (11), 1285-1292.

132. Safo, M. K.; Musayev, F. N.; Wu, S. H.; Abraham, D. J.; Ko, T. P., Structure of tetragonal crystals of human erythrocyte catalase. *Acta Crystallogr. Sect. D-Biol. Crystallogr.* **2001**, *57*, 1-7.

133. Banci, L.; Benedetto, M.; Bertini, I.; Del Conte, R.; Piccioli, M.; Viezzoli, M. S., Solution structure of reduced monomeric Q133M2 copper, zinc superoxide dismutase (SOD). Why is SOD a dimeric enzyme? *Biochemistry* **1998**, *37* (34), 11780-11791.